Journal of Scientific Computing (2019) 78:1660–1690
https://doi.org/10.1007/s10915-018-0819-2

CrossMark

Local Discontinuous Galerkin Methods with Generalized Alternating Numerical Fluxes for Two-dimensional Linear Sobolev Equation

Di Zhao[1] · **Qiang Zhang**[1]

Received: 18 April 2018 / Revised: 19 July 2018 / Accepted: 27 August 2018 /
Published online: 1 September 2018

Abstract
In this paper we present an efficient and high-order numerical method to solve two-dimensional linear Sobolev equations, which is based on the local discontinuous Galerkin (LDG) method with the upwind-biased fluxes and generalized alternating fluxes. A weak stability is given for both schemes, and a strong stability is established if the initial solutions exactly satisfy the elemental discontinuous Galerkin discretization. Moreover, the sharp error estimate in L^2-norm is established, by an elaborate application of the generalized Gauss–Radau projection. A fully-discrete LDG scheme is also considered, where the third-order explicit TVD Runge–Kutta algorithm is adopted. Finally some numerical experiments are given.

Keywords Sobolev equation · Local discontinuous Galerkin method · Upwind-biased/generalized alternating numerical fluxes · Stability and error estimate · Generalized Gauss–Radau projection

1 Introduction

In this paper we present and analyze an efficient numerical method to solve the multi-dimensional Sobolev equation, where a third-order mixed derivative is included. The linear constant equation in two-dimensional space can be written in the form

$$U_t + c_1 U_x + c_2 U_y - \varepsilon(U_{xx} + U_{yy}) = \mu(U_{xxt} + U_{yyt}), \tag{1.1}$$

D. Zhao: Supported by CNSF with Grant No. 11671193. Q. Zhang: Supported by CNSF with Grant Nos. 11671193 and 11571290.

✉ Qiang Zhang
qzh@nju.edu.cn

Di Zhao
DG1621025@smail.nju.edu.cn

1 Department of Mathematics, Nanjing University, Nanjing 210093, Jiangsu Province, People's Republic of China

where $\boldsymbol{c} = (c_1, c_2)$ is the convection speed, and $\varepsilon \geq 0$ and $\mu > 0$ are respectively the diffusion and dispersion coefficients. This type of equation is also called pseudo-parabolic equation, which appears in engineering fields such as, for instance, flows of fluids through fissured rock, heat conduction involving a thermodynamic temperature and a conductive temperature, and quasi-stationary processes in semiconductors (see, e.g. [1,11]). For a discussion of existence and uniqueness results, please see references [9,12].

Up to now, a large number of important works on finite element method have been implemented for the resolution of this type of equation, for example, the standard finite element method [2,10,13,18], the mixed finite element method [15,19], and the local discontinuous Galerkin (LDG) method [14,23]. The LDG method was firstly introduced by Cockburn and Shu [7], in the 1980's, to solve the convection–diffusion problems, inspired by the work of Bassi and Rebay [3] for the compressible Navier–Stokes equation. It is an extension of the Runge–Kutta discontinuous Galerkin method [5,6] for nonlinear hyperbolic systems. Till now, many works on the LDG method for those partial differential equations with higher order derivatives [16,20–22] were carried out. For a fairly complete set of references on this methods, see the review paper by Cockburn and Shu [7,8].

In this paper we continue the works in [14,23], in which the authors have discussed the semi-discrete LDG scheme and two fully-discrete LDG schemes for one-dimensional Sobolev equations. However, they only considered one-dimensional problem and a special definition of numerical flux. Hence, we would like here to extend the above LDG schemes to solve two-dimensional Sobolev equations, and enlarge the range of definitions of numerical fluxes at the same time. Namely, we adopt the generalized alternating fluxes for diffusion and dispersion, and independently adopt the upwind-biased fluxes for convection. These types of numerical fluxes are more flexible for linear equations with varying coefficients and even nonlinear equations. Similar discussions have been carried out in many literatures, for example, in [4,17] for hyperbolic equation and convection–diffusion equation, respectively.

In this paper, we will firstly give the semi-discrete LDG scheme with two setting of initial solutions. Then, we present a fully-discrete LDG scheme, where the third order explicit total variation diminishing Runge–Kutta (TVDRK) time-marching is coupled with. Almost the same as in [14,23], the advantages in numerical implementation are preserved in this paper. Owing to the special definition of first-order differential system [see (2.8)], not only the time-updating can be done directly and efficiently for the freedom of numerical solution, but also the existing coding of LDG method to solve an elliptic problem can be easily applied.

Furthermore, the LDG schemes are proved to have strong stability in μ-norm (see Theorems 3.1 and 5.1), if the initial solution (with respect to the prime variable and two auxiliary variables) exactly satisfies the elemental DG discretization. As a comparison, the standard L^2-projection for two auxiliary variables is also adopted in this paper to simplify the definition and implementation of initial solution. Although the strong stability does not hold any more, there still holds a good stability in weak sense (see Lemmas 3.5 and 5.3).

The main highlight in this paper is establishing the sharp error estimate in a uniform framework (see Theorems 4.1 and 5.2). Firstly, the results show explicitly the effect when the parameters in numerical fluxes are not the same. Secondly, the bounding constant does not depend on the reciprocal of two coefficients ε and μ, after removing the effect of the regularity of exact solution. As a consequence, the accuracy order is always optimal when the parameters in numerical fluxes are the same, and a reduction of accuracy order might happen sometimes. Namely, the accuracy order is only achieved quasi-optimal when the maximum of ε and μ is in the same order of the mesh size, and the parameters in each space direction are different. The kernel tool in error estimate is the elaborate application of the generalized Gauss–Radau (GGR) projections, which involves a combination of the prime variable and the other auxiliary variables. In this analysis process, the super-convergence of the projection error, corresponding to a special GGR projection, is used many times.

The paper is organized as follows. In Sect. 2, we present the semi-discrete LDG scheme for problem (1.1), where the periodic boundary condition is considered. In Sects. 3 and 4, we present the stability results and error estimates for the semi-discrete scheme with two setting of initial solutions. In Sect. 5, we extend the above works to the fully-discrete scheme with the third-order explicit TVDRK time-marching. Some numerical experiments are given in Sect. 6, and some technical proofs are given in "Appendix".

2 LDG Scheme

In this section we define the semi-discrete LDG scheme for the Sobolev equation (1.1). For simplicity, we take the space domain $\Omega = (0, 2\pi)^2$ with the periodic boundary condition. The time interval is taken $[0, T]$, where $T > 0$ is the final time. In addition, we assume that both c_1 and c_2 are nonnegative.

2.1 Finite Element Space and Notations

Let $\Omega_h = \{K_{ij}\}$ be a quasi-uniform partition of given domain Ω with rectangular element $K_{ij} = I_i \times J_j$, where $i = 1, 2, \ldots, N_x$ and $j = 1, 2, \ldots, N_y$. Here both N_x and N_y are positive integers, and $I_i = (x_{i-1/2}, x_{i+1/2})$ and $J_j = (y_{j-1/2}, y_{j+1/2})$. Let $h_i^x = x_{i+1/2} - x_{i-1/2}$ and $h_j^y = y_{j+1/2} - y_{j-1/2}$ be the length and width of K_{ij}, and define $h = \max_{i,j}\{h_i^x, h_j^y\}$ as the mesh size. The associated finite element space is defined as

$$V_h = \{v(x, y) : v|_K \in \mathcal{Q}_k(K) \text{ for any } K \in \Omega_h\}, \tag{2.1}$$

where $\mathcal{Q}_k(K)$ represents the space of polynomials on K of degree at most $k > 0$ in each variable. Note that the function $v \in V_h$ is allowed to have discontinuities across the element interfaces. Following [4], we use

$$[\![v]\!]_{i+\frac{1}{2},y} = v^+_{i+\frac{1}{2},y} - v^-_{i+\frac{1}{2},y}, \quad \{\!\{v\}\!\}^{\alpha,y}_{i+\frac{1}{2},y} = \alpha v^-_{i+\frac{1}{2},y} + (1-\alpha) v^+_{i+\frac{1}{2},y}, \tag{2.2a}$$

$$[\![v]\!]_{x,j+\frac{1}{2}} = v^+_{x,j+\frac{1}{2}} - v^-_{x,j+\frac{1}{2}}, \quad \{\!\{v\}\!\}^{x,\alpha}_{x,j+\frac{1}{2}} = \alpha v^-_{x,j+\frac{1}{2}} + (1-\alpha) v^+_{x,j+\frac{1}{2}}, \tag{2.2b}$$

to represent the jumps and the weighted averages on each vertical edges and horizontal edges, respectively, where α is a given weight, and

$$v^\pm_{i+\frac{1}{2},y} = \lim_{x \to x^\pm_{i+1/2}} v(x, y), \quad v^\pm_{x,j+\frac{1}{2}} = \lim_{y \to y^\pm_{j+1/2}} v(x, y) \tag{2.3}$$

are the traces along four directions. It is worthy to note that the above notations can be extended to the broken Sobolev space

$$H^1(\Omega_h) = \{\varphi(x, y) \colon \varphi|_K \in H^1(K) \text{ for any } K \in \Omega_h\}, \tag{2.4}$$

which contains the discontinuous finite element space V_h.

For convenience, some notations are used. We introduce the following bilinear functionals along two space directions

$$\mathcal{H}_1^{\alpha}(\varphi,\psi)=\int_{\Omega_h}\varphi\psi_x\mathrm{d}x\mathrm{d}y+\sum_{i=1}^{N_x}\sum_{j=1}^{N_y}\int_{J_j}\{\!\{\varphi\}\!\}_{i+\frac12,y}^{\alpha,y}[\![\psi]\!]_{i+\frac12,y}\mathrm{d}y, \tag{2.5a}$$

$$\mathcal{H}_2^{\alpha}(\varphi,\psi)=\int_{\Omega_h}\varphi\psi_y\mathrm{d}x\mathrm{d}y+\sum_{i=1}^{N_x}\sum_{j=1}^{N_y}\int_{I_i}\{\!\{\varphi\}\!\}_{x,j+\frac12}^{x,\alpha}[\![\psi]\!]_{x,j+\frac12}\mathrm{d}x, \tag{2.5b}$$

where both φ and ψ belong to $H^1(\Omega_h)$. Here the subscripts, 1 and 2, represent the elemental DG discretization of derivatives along x- and y-directions respectively. Let Γ_h^1 and Γ_h^2 be the vertical edges and horizontal edges of every elements, respectively, and define the corresponding inner products

$$\left(\varphi,\psi\right)_{\Gamma_h^1}=\frac12\sum_{i=1}^{N_x}\sum_{j=1}^{N_y}\int_{J_j}\left[\varphi_{i+\frac12,y}^{+}\psi_{i+\frac12,y}^{+}+\varphi_{i+\frac12,y}^{-}\psi_{i+\frac12,y}^{-}\right]\mathrm{d}y, \tag{2.6a}$$

$$\left(\varphi,\psi\right)_{\Gamma_h^2}=\frac12\sum_{i=1}^{N_x}\sum_{j=1}^{N_y}\int_{I_i}\left[\varphi_{x,j+\frac12}^{+}\psi_{x,j+\frac12}^{+}+\varphi_{x,j+\frac12}^{-}\psi_{x,j+\frac12}^{-}\right]\mathrm{d}x. \tag{2.6b}$$

The associated norms are denoted by $\|\psi\|_{\Gamma_h^\kappa}=(\psi,\psi)_{\Gamma_h^\kappa}^{1/2}$ for $\kappa=1,2$. We also use $(\cdot,\cdot)$ to represent the inner product in $L^2(\Omega_h)$, with the associated L^2-norm $\|\cdot\|$.

In what follows, the argument in a function will be omitted; however, the time argument may be pointed out if necessary. Throughout this paper, we use κ to represent the spatial direction, which is always taken from $\{1,2\}$.

2.2 Semi-discrete Scheme

Following the idea in [14,23], we introduce five auxiliary variables

$$W=U_t,\quad \boldsymbol{P}=(P_1,P_2)=\nabla W,\quad \boldsymbol{Q}=(Q_1,Q_2)=\nabla U, \tag{2.7}$$

and write Eq. (1.1) into the equivalent first-order differential system

$$U_t=W,\quad \boldsymbol{Q}_t=\boldsymbol{P}, \tag{2.8a}$$

$$W+\nabla\cdot(\boldsymbol{F}(U)-\varepsilon\boldsymbol{Q}-\mu\boldsymbol{P})=0,\qquad \boldsymbol{P}=\nabla W, \tag{2.8b}$$

where $\boldsymbol{F}(U)=(c_1U,c_2U)$ is the convection flux. Note that the second equation in (2.8a) is the key point in this paper, which is directly derived from (2.7). By replacing the original definition $\boldsymbol{Q}=\nabla U$ with this equation, we can easily design the numerical fluxes in the LDG scheme, and achieve the advantages in numerical implementations; seeing Remark 5.1.

Denote the exact solution of (2.8) by $\boldsymbol{Z}=(\boldsymbol{Z}_{uq},\boldsymbol{Z}_{wp})=(U,\boldsymbol{Q},W,\boldsymbol{P})$. Correspondingly, denote the approximation solution by $\boldsymbol{z}=(\boldsymbol{z}_{uq},\boldsymbol{z}_{wp})=(u,\boldsymbol{q},w,\boldsymbol{p})$, in which each component belongs to V_h at any time. Here $\boldsymbol{q}=(q_1,q_2)$ and $\boldsymbol{p}=(p_1,p_2)$. The semi-discrete

LDG scheme of (1.1) is then defined as follows: find $z = z(\cdot, t)$ for $t \in (0, T]$, such that

$$\Big(u_t, v_u\Big) = \Big(w, v_u\Big), \tag{2.9a}$$

$$\Big((q_\kappa)_t, v_{q_\kappa}\Big) = \Big(p_\kappa, v_{q_\kappa}\Big), \tag{2.9b}$$

$$\Big(w, v_w\Big) - \sum_{\kappa=1}^{2}\Big[c_\kappa \mathcal{H}_\kappa^{\gamma_\kappa}(u, v_w) - \varepsilon \mathcal{H}_\kappa^{1-\theta_\kappa}(q_\kappa, v_w) - \mu \mathcal{H}_\kappa^{1-\theta_\kappa}(p_\kappa, v_w)\Big] = 0, \tag{2.9c}$$

$$\Big(p_\kappa, v_{p_\kappa}\Big) + \mathcal{H}_\kappa^{\theta_\kappa}(w, v_{p_\kappa}) = 0, \tag{2.9d}$$

hold for any test functions v_u, v_{q_κ}, v_w and $v_{p_\kappa} \in V_h$. In (2.9c) and (2.9d), those weighted averages emerged in the element boundaries are called the numerical fluxes. They depend on the parameters γ_κ and θ_κ. Since $c_\kappa \geq 0$, we would like to take

$$\gamma_\kappa > 1/2, \quad \theta_\kappa \neq 1/2, \tag{2.10}$$

in this paper. Actually, $\gamma_\kappa = 1/2$ and $\theta_\kappa = 1/2$ are admissible. However, we do not care about this case in this paper. If $\gamma_\kappa = 1$, the purely upwind flux is used for convection. If $\theta_\kappa \in \{0, 1\}$, the purely alternating fluxes are used for diffusion and dispersion. Hence, the numerical fluxes considered in this paper are called the upwind-biased flux [17], and the generalized alternating flux [4], respectively. For convenience, they are collectively called the generalized alternating fluxes.

Remark 2.1 It is worthy to mention that $\gamma_\kappa \neq \theta_\kappa$ is admissible in this paper. However, the numerical fluxes for diffusion and dispersion must be well organized, like (2.9c) and (2.9d), to ensure the good stability and high-order accuracy.

To ensure the sharp (quasi or quasi-optimal) error estimate, the initial solutions should be carefully given also. In this paper, we define $u(0)$ as the GGR projection of $U(0)$, namely

$$u(0) = \mathbb{Q}^{\theta_1,\theta_2} U(0), \tag{2.11}$$

where θ_1 and θ_2 are the parameters used in the scheme. The detailed definition will be given in Sect. 4.1. As for $q_\kappa(0)$, we mainly consider two definitions in this paper:

1. One is the standard L^2-projection of $Q_\kappa(0)$, namely it satisfies $(q_\kappa(0), v) = (Q_\kappa(0), v)$ for any $v \in V_h$. Equivalently, it is defined as the unique element in V_h such that
$$\Big(q_\kappa(0), v\Big) + \mathcal{H}_\kappa^{\theta_\kappa}(U(0), v) = 0, \ \forall\, v \in V_h. \tag{2.12a}$$
Here $Q_\kappa(0)$ is the derivative of $U(0)$ along the related spatial direction.
2. The other is defined as the unique element in V_h satisfying the variation form
$$\Big(q_\kappa(0), v\Big) + \mathcal{H}_\kappa^{\theta_\kappa}(u(0), v) = 0, \ \forall\, v \in V_h. \tag{2.12b}$$
Namely, the numerical solution exactly satisfies the elemental DG discretization.

Although definition 1 can be easily implemented, it is not able to provide the strong stability as definition 2; see Theorem 3.1.

Till now, we complete the definition of the semi-discrete of LDG scheme. Throughout this paper, the LDG methods with two definitions of initial solutions are called the LDG(I) scheme and the LDG(II) scheme, respectively.

2.3 A Compact and General Description

For convenience of presentation and analysis, we introduce two notations $\boldsymbol{\Psi}_{uq}$ and $\boldsymbol{\Psi}_{wp}$, and extend the variation form (2.9) into the non-homogeneous case. It can be written into a compact form

$$\Big\langle (z_{uq})_t, \boldsymbol{v}_{uq} \Big\rangle = \Big\langle z_{wp}, \boldsymbol{v}_{uq} \Big\rangle + \Big\langle \boldsymbol{\Psi}_{uq}, \boldsymbol{v}_{uq} \Big\rangle, \quad \forall\, \boldsymbol{v}_{uq} = (v_u, v_{q_1}, v_{q_2}) \in (V_h)^3, \tag{2.13a}$$

$$\Big\langle z_{wp}, \boldsymbol{v}_{wp} \Big\rangle = \mathcal{H}(z, \boldsymbol{v}_{wp}) + \Big\langle \boldsymbol{\Psi}_{wp}, \boldsymbol{v}_{wp} \Big\rangle, \quad \forall\, \boldsymbol{v}_{wp} = (v_w, v_{p_1}, v_{p_2}) \in (V_h)^3, \tag{2.13b}$$

in which both $\boldsymbol{\Psi}_{uq} = (\Psi_u, \Psi_{q_1}, \Psi_{q_2})$ and $\boldsymbol{\Psi}_{wp} = (\Psi_w, \Psi_{p_1}, \Psi_{p_2})$ are the given maps, continuously mapping the time $t \in (0, T]$ into $(V_h)^3$. Here

$$\mathcal{H}(z, \boldsymbol{v}_{wp}) = \sum_{\kappa=1}^{2} \Big[c_\kappa \mathcal{H}_\kappa^{\gamma_\kappa}(u, v_w) - \varepsilon \mathcal{H}_\kappa^{1-\theta_\kappa}(q_\kappa, v_w) - \mu \mathcal{H}_\kappa^{1-\theta_\kappa}(p_\kappa, v_w) - \mu \mathcal{H}_\kappa^{\theta_\kappa}(w, v_{p_\kappa}) \Big] \tag{2.14}$$

is the LDG discretization in space, and $\langle \cdot, \cdot \rangle$ is defined in the form like

$$\Big\langle z_{wp}, \boldsymbol{v}_{wp} \Big\rangle = \Big(w, v_w \Big) + \mu \Big(p_1, v_{p_1} \Big) + \mu \Big(p_2, v_{p_2} \Big). \tag{2.15}$$

Note that $\langle \cdot, \cdot \rangle$ is an inner product in $[L^2(\Omega)]^3$, since $\mu > 0$. The associated norm is denoted by $\| \cdot \|_\mu = \langle \cdot, \cdot \rangle^{1/2}$. For both the LDG(I) scheme and the LDG(II) scheme, it is easy to see $\boldsymbol{\Psi}_{uq} = \boldsymbol{\Psi}_{wp} = 0$. These notations will be mainly used in the error estimate.

The definition of initial solutions can be written into a uniform relationship. Namely, there exists a unique element $S_\kappa(0) \in V_h$, for the initial solution $z_{uq}(0) \in (V_h)^3$, such that

$$\Big(q_\kappa(0), v \Big) + \mathcal{H}_\kappa^{\theta_\kappa}(u(0), v) = \Big(S_\kappa(0), v \Big), \quad \forall\, v \in V_h. \tag{2.16}$$

For the LDG(II) scheme, it is easy to see $S_\kappa(0) = 0$. However, for the LDG(I) scheme, we have $S_\kappa(0) \neq 0$ in general.

3 Stability Analysis

In this section we present the stability results for the above two semi-discrete LDG schemes. In what follows, we use C to denote those generic positive constants, independent of h, ε^{-1}, μ^{-1} and T.

3.1 Properties About DG Discretization

Now we give some elemental properties about the DG discretization with respect to the first-order derivative, where an arbitrary parameter α is involved.

The first one is the accurately skew-symmetric construction for generalized alternating numerical fluxes, and the second one is the approximating skew-symmetric property, mainly used for the convection.

Lemma 3.1 *For any φ and ψ in $H^1(\Omega_h)$, there holds*

$$\mathcal{H}_\kappa^{1-\alpha}(\varphi, \psi) + \mathcal{H}_\kappa^{\alpha}(\psi, \varphi) = 0. \tag{3.1}$$

Lemma 3.2 *For any φ and ψ in $H^1(\Omega_h)$, there holds*

$$\mathcal{H}_\kappa^\alpha(\psi,\varphi)+\mathcal{H}_\kappa^\alpha(\varphi,\psi)=-(2\alpha-1)\Big([\![\varphi]\!],[\![\psi]\!]\Big)_{\Gamma_h^\kappa}, \tag{3.2}$$

which implies $\mathcal{H}_\kappa^\alpha(\varphi,\varphi)=-\frac{1}{2}(2\alpha-1)\|[\![\varphi]\!]\|^2_{\Gamma_h^\kappa}$.

The last one is the boundedness in V_h, due to the Cauchy–Schwarz inequality and the inverse properties

$$\|\nabla v\|\le \nu h^{-1}\|v\|,\quad \|v\|_{\Gamma_h}\le \nu h^{-1/2}\|v\|,\quad \forall v\in V_h. \tag{3.3}$$

Here $\Gamma_h=\Gamma_h^1\cup\Gamma_h^2$, and $\|\cdot\|_{\Gamma_h}=(\|\cdot\|^2_{\Gamma_h^1}+\|\cdot\|^2_{\Gamma_h^2})^{1/2}$. Note that $\nu>0$ is the inverse constant solely depending on the degree k.

Lemma 3.3 *For any φ and ψ in V_h, there holds*

$$\mathcal{H}_\kappa^\alpha(\varphi,\psi)\le Mh^{-1}\|\varphi\|\|\psi\|, \tag{3.4}$$

where the bounding constant $M>0$ solely depends on the inverse constant.

Similar discussions can be found in many literatures, for example [24], so the proofs are omitted here.

3.2 An Implicit Relationship

For convenience of presentation, we would like to introduce some notations. Firstly let $\mathcal{H}_\kappa^{\theta_\kappa}\Psi_u$ be the unique Rietz presentation in V_h such that $(\mathcal{H}_\kappa^{\theta_\kappa}\Psi_u,v)=\mathcal{H}_\kappa^{\theta_\kappa}(\Psi_u,v)$ holds for any $v\in V_h$, and then define

$$Y_\kappa(t)=\Psi_{p_\kappa}(t)+\Psi_{q_\kappa}(t)+\mathcal{H}_\kappa^{\theta_\kappa}\Psi_u(t),\quad t\in(0,T], \tag{3.5a}$$

which also belongs to V_h at any time. Roughly speaking, this term represents the instantaneous change of the residual between the auxiliary variable q_κ and one spatial derivative of u in the DG framework. Taking account on relationship (2.16) in the initial solutions, the accumulation of Y_κ over the time interval $[0,t]$ is defined as

$$\Phi_\kappa(t)=\int_0^t Y_\kappa(s)\mathrm{d}s+S_\kappa(0),\quad t\in[0,T]. \tag{3.5b}$$

If no confusion, the argument t will be omitted.

Lemma 3.4 *For $t\in[0,T]$, the solution of (2.13) satisfies*

$$\Big(q_\kappa,v\Big)+\mathcal{H}_\kappa^{\theta_\kappa}(u,v)=\Big(\Phi_\kappa,v\Big),\quad \forall v\in V_h. \tag{3.6}$$

Proof If $t=0$, the conclusion holds water due to (2.16). Below we take $\kappa=1$ as an example to prove this lemma for any time $t>0$. Since both the trial functions and the test functions are in the same finite element space, it is easy to obtain from (2.13a) that

$$(z_{uq})_t=z_{wp}+\boldsymbol{\Psi}_{uq},\quad t\in(0,T]. \tag{3.7}$$

Plugging it into (2.13b) with the test function $\boldsymbol{v}_{wp}=(0,v,0)$, and integrating over the time interval $[0,t]$, we can obtain (3.6) by using (2.16) again. □

This lemma will be used serval times in this paper, which implies the essential property in the LDG scheme. It also explicitly shows the affection of the initial solutions. For example, for the LDG(II) scheme, it follows from this lemma that

$$\Big(q_\kappa, v\Big) + \mathcal{H}_\kappa^{\theta_\kappa}(u, v) = 0, \quad \forall\, v \in V_h,$$

since $\boldsymbol{\Psi}_{uq} = \boldsymbol{\Psi}_{wp} = 0$ and $S_\kappa(0) = 0$. This identity shows the derivative relation between u and q_κ in the DG framework, consistent with the last definition in (2.7).

3.3 Stability Results

To carry out the stability analysis for the above LDG schemes, we firstly take $\boldsymbol{v}_{wp} = (u, 0, 0)$ in (2.13b), and then take $v = \varepsilon q_\kappa$ and $v = \mu p_\kappa$ in (3.6), respectively. The sum of three resulted equalities yields that

$$R_1 + R_2 + R_3 = \Big(\Psi_w, u\Big) + \sum_{\kappa=1}^{2}\Big(\Phi_\kappa, \varepsilon q_\kappa + \mu p_\kappa\Big), \tag{3.8}$$

where

$$R_1 = \Big(w, u\Big) + \mu\sum_{\kappa=1}^{2}\Big(q_\kappa, p_\kappa\Big), \tag{3.9a}$$

$$R_2 = \varepsilon\sum_{\kappa=1}^{2}\Big[\mathcal{H}_\kappa^{1-\theta_\kappa}(q_\kappa, u) + \mathcal{H}_\kappa^{\theta_\kappa}(u, q_\kappa)\Big] + \mu\sum_{\kappa=1}^{2}\Big[\mathcal{H}_\kappa^{1-\theta_\kappa}(p_\kappa, u) + \mathcal{H}_\kappa^{\theta_\kappa}(u, p_\kappa)\Big], \tag{3.9b}$$

$$R_3 = \varepsilon\sum_{\kappa=1}^{2}\Big(q_\kappa, q_\kappa\Big) - \sum_{\kappa=1}^{2} c_\kappa \mathcal{H}_\kappa^{\gamma_\kappa}(u, u). \tag{3.9c}$$

It follows from (3.7) that $R_1 = \langle (z_{uq})_t, z_{uq}\rangle - \langle \boldsymbol{\Psi}_{uq}, z_{uq}\rangle$. Using Lemma 3.1 twice yields $R_2 = 0$. Owing to Lemma 3.2, we get

$$R_3 = \varepsilon\|\boldsymbol{q}\|^2 + \frac{1}{2}\sum_{\kappa=1}^{2} c_\kappa(2\gamma_\kappa - 1)\|[\![u]\!]\|^2_{\Gamma_h^\kappa} \equiv \mathcal{S}(t), \tag{3.10}$$

where $\|\boldsymbol{q}\|^2 = \|q_1\|^2 + \|q_2\|^2$. Since $\gamma_\kappa > 1/2$, the term $\mathcal{S} = \mathcal{S}(t) \geq 0$ explicitly shows the numerical stability of this method. Substituting the above conclusions into (3.8), we obtain the energy equation

$$\Big\langle (z_{uq})_t, z_{uq}\Big\rangle + \mathcal{S} = \Big(\Psi_w, u\Big) + \Big\langle \boldsymbol{\Psi}_{uq}, z_{uq}\Big\rangle + \sum_{\kappa=1}^{2}\Big(\Phi_\kappa, \varepsilon q_\kappa + \mu p_\kappa\Big), \tag{3.11}$$

for any time.

As a direct application of this conclusion, we have the following theorem.

Theorem 3.1 *For the semi-discrete LDG(II) scheme, there holds the strong stability in the sense*

$$\|u(t)\|^2 + \mu\|\boldsymbol{q}(t)\|^2 \leq \|u(0)\|^2 + \mu\|\boldsymbol{q}(0)\|^2, \quad t > 0. \tag{3.12}$$

Proof Since $\boldsymbol{\Psi}_{uq} = \boldsymbol{\Psi}_{wp} = 0$ and $S_\kappa(0) = 0$ at this moment, there holds $\Phi_\kappa \equiv 0$. Then it follows from (3.11) that

$$\frac{\mathrm{d}}{\mathrm{d}t}\Big[\|u\|^2 + \mu\|\boldsymbol{q}\|^2\Big] \le 0, \quad t > 0. \tag{3.13}$$

Hence the theorem is proved. □

Next we continue to estimate the right-hand side of (3.11) for general case, in which the main trouble comes from the last term. Making an integration over the time interval $[0, t]$, we can yield

$$\frac{1}{2}\|z_{uq}(t)\|_\mu^2 + \int_0^t \mathcal{S}(s)\mathrm{d}s = \frac{1}{2}\|z_{uq}(0)\|_\mu^2 + \sum_{\kappa=1}^{2} G_{1\kappa}(t) + \sum_{\kappa=1}^{2} G_{2\kappa}(t) + G_3(t), \tag{3.14}$$

where

$$G_{1\kappa}(t) = \varepsilon\int_0^t \Big(\Phi_\kappa(s), q_\kappa(s)\Big)\mathrm{d}s, \quad G_{2\kappa}(t) = \mu\int_0^t \Big(\Phi_\kappa(s), p_\kappa\Big)\mathrm{d}s, \tag{3.15a}$$

and

$$G_3(t) = \int_0^t \Big[\Big(\Psi_w(s), u(s)\Big) + \Big\langle \boldsymbol{\Psi}_{uq}(s), z_{uq}(s)\Big\rangle\Big]\mathrm{d}s. \tag{3.15b}$$

A simple application of Cauchy–Schwarz inequality yields

$$G_{1\kappa}(t) \le \frac{\varepsilon}{2}\int_0^t \|\Phi_\kappa(s)\|^2\mathrm{d}s + \frac{\varepsilon}{2}\int_0^t \|q_\kappa(s)\|^2\mathrm{d}s, \tag{3.16}$$

$$G_3(t) \le CT\int_0^t \Big[\|\Psi_w(s)\|^2 + \|\boldsymbol{\Psi}_{uq}(s)\|_\mu^2\Big]\mathrm{d}s + \frac{C}{T}\int_0^t \|z_{uq}(s)\|_\mu^2\mathrm{d}s. \tag{3.17}$$

However, we need more treatment on the remaining term $G_{2\kappa}(t)$. Owing to (3.7), an integration by part in time yields

$$\begin{aligned} G_{2\kappa}(t) &= \mu\int_0^t \Big(\Phi_\kappa(s), (q_\kappa)_t(s) - \Psi_{q_\kappa}(s)\Big)\mathrm{d}s \\ &= \mu\Big(\Phi_\kappa(s), q_\kappa(s)\Big)\Big|_{s=0}^{s=t} - \mu\int_0^t \Big(Y_\kappa(s), q_\kappa(s)\Big)\mathrm{d}s - \mu\int_0^t \Big(\Phi_\kappa(s), \Psi_{q_\kappa}(s)\Big)\mathrm{d}s, \end{aligned}$$

in which three terms on the right-hand side are denoted in order by $G_{2\kappa}^{(1)}$, $G_{2\kappa}^{(2)}$, and $G_{2\kappa}^{(3)}$. Some applications of Cauchy–Schwarz inequality yield

$$G_{2\kappa}^{(1)} \le \frac{1}{4}\mu\|q_\kappa(t)\|^2 + \frac{1}{4}\mu\|q_\kappa(0)\|^2 + C\mu\Big[\|\Phi_\kappa(t)\|^2 + \|\Phi_\kappa(0)\|^2\Big], \tag{3.18a}$$

$$G_{2\kappa}^{(2)} \le C\mu\Big[T\int_0^t \|Y_\kappa(s)\|^2\mathrm{d}s + \frac{1}{T}\int_0^t \|q_\kappa(s)\|^2\mathrm{d}s\Big], \tag{3.18b}$$

$$G_{2\kappa}^{(3)} \le C\mu\Big[\int_0^t \|\Phi_\kappa(s)\|^2\mathrm{d}s + \int_0^t \|\Psi_{q_\kappa}(s)\|^2\mathrm{d}s\Big]. \tag{3.18c}$$

Summing up the above inequalities into (3.14), and noticing definition (3.10), we have

$$\frac{1}{4}\|z_{uq}(t)\|_\mu^2 + \frac{1}{2}\int_0^t \mathcal{S}(s)\mathrm{d}s \le \frac{C}{T}\int_0^t \|z_{uq}(s)\|_\mu^2\mathrm{d}s + C\Pi_1(t) + C\Pi_2(t) + C\Pi_3(t), \tag{3.19}$$

holds for any time, where

$$\Pi_1(t) = \int_0^t \Big[T\|\Psi_w(s)\|^2 + (1+T)\|\boldsymbol{\Psi}_{uq}(s)\|_\mu^2\Big]\mathrm{d}s, \tag{3.20a}$$

$$\Pi_2(t) = \sum_{\kappa=1}^{2}\int_0^t \Big[T\mu\|Y_\kappa(s)\|^2 + (\mu+\varepsilon)\|\Phi_\kappa(s)\|^2\Big]\mathrm{d}s, \tag{3.20b}$$

$$\Pi_3(t) = \|z_{uq}(0)\|_\mu^2 + \mu\sum_{\kappa=1}^{2}\Big[\|\Phi_\kappa(t)\|^2 + \|\Phi_\kappa(0)\|^2\Big]. \tag{3.20c}$$

Now using the Gronwall's inequality can yield the following lemma.

Lemma 3.5 *For any time $t \in [0, T]$, there holds*

$$\|z_{uq}(t)\|_\mu^2 \le C\Pi_1(t) + C\Pi_2(t) + C\Pi_3(t), \tag{3.21}$$

where the bounding constant $C > 0$ is independent of h, ε^{-1}, μ^{-1} and T.

This lemma implies a weak stability for the semi-discrete LDG(I) scheme, since $\boldsymbol{\Psi}_{uq} = \boldsymbol{\Psi}_{wp} = 0$ and $Y_\kappa \equiv 0$ still hold at this moment. Even though $\Phi_\kappa = S_\kappa(0) \neq 0$ may cause some negative affection on the stability, it can also be bounded by the given initial solution. However, the reciprocal of the mesh size might be involved in the bounding constant. This is the reason why the above result is called the weak stability.

4 Error Estimate

In this section, we establish the *sharp* error estimate of the above two semi-discrete LDG schemes. The conclusion is stated as follows, and the proof will be given in the next three subsections.

Theorem 4.1 *Assume that the exact solution satisfies $U \in W^{1,\infty}(H^{k+2})$, whose regularity boundedness (the norm in this space–time Sobolev space) is denoted by A. Then we have*

$$\Big[\|U-u\|_{L^\infty(L^2)}^2 + \mu\|\boldsymbol{Q}-\boldsymbol{q}\|_{L^\infty(L^2)}^2\Big]^{\frac{1}{2}} \le CA(1+T)\Big[h^{k+1} + \varrho h^k\Big], \tag{4.1}$$

where

$$\varrho = \Big[\sqrt{\varepsilon}+\sqrt{\mu}\Big]\sum_{\kappa=1}^{2}\min\left(1, \frac{c_\kappa h}{\varepsilon}, \frac{c_\kappa h}{\mu}\right)|\theta_\kappa - \gamma_\kappa|, \tag{4.2}$$

and the bounding constant $C > 0$ is independent of h, ε^{-1}, μ^{-1} and T.

Here and below some notations and norms of space–time Sobolev space are used, where the space domain Ω and the time interval $[0, T]$ are omitted for convenience.

Theorem 4.1 shows the sharp error estimate for the prime variable U in the L^2-norm. If $\theta_\kappa = \gamma_\kappa$, the order is always optimal. Otherwise, if $\theta_\kappa \neq \gamma_\kappa$, it follows from the definition of ϱ that a half-order reduction may happen when $\max(\varepsilon, \mu) = \mathcal{O}(h)$.

4.1 Original GGR Projection

The kernel tool in error estimate is the GGR projection. Let α_1 and α_2 be two arbitrary parameters. For any smooth function $g = g(x, y)$, the original GGR projection $\mathbb{Q}^{\alpha_1,\alpha_2} g$ is defined as follows, depending on the values of α_1 and α_2.

- If $\alpha_1 \neq \frac{1}{2}$ and $\alpha_2 \neq \frac{1}{2}$, the projection error $\eta_g = g - \mathbb{Q}^{\alpha_1,\alpha_2} g$ satisfies

$$\int_{K_{ij}} \eta_g v \, \mathrm{d}x \, \mathrm{d}y = 0, \quad \forall\, v \in \mathcal{Q}_{k-1}(K_{ij}), \tag{4.3a}$$

$$\int_{J_j} \{\!\{\eta_g\}\!\}^{\alpha_1,y}_{i+\frac{1}{2},y} v_{i+\frac{1}{2},y} \, \mathrm{d}y = 0, \quad \forall\, v \in \mathcal{P}_{k-1}(J_j), \tag{4.3b}$$

$$\int_{I_i} \{\!\{\eta_g\}\!\}^{x,\alpha_2}_{x,j+\frac{1}{2}} v_{x,j+\frac{1}{2}} \, \mathrm{d}x = 0, \quad \forall\, v \in \mathcal{P}_{k-1}(I_i), \tag{4.3c}$$

$$\{\!\{\eta_g\}\!\}^{\alpha_1,\alpha_2}_{i+\frac{1}{2},j+\frac{1}{2}} = 0, \tag{4.3d}$$

where

$$\begin{aligned}\{\!\{\eta_g\}\!\}^{\alpha_1,\alpha_2}_{i+\frac{1}{2},j+\frac{1}{2}} &= \alpha_1\alpha_2\eta_g(x^-_{i+\frac{1}{2}}, y^-_{j+\frac{1}{2}}) + \alpha_1(1-\alpha_2)\eta_g\left(x^-_{i+\frac{1}{2}}, y^+_{j+\frac{1}{2}}\right)\\ &\quad + (1-\alpha_1)\alpha_2\eta_g\left(x^+_{i+\frac{1}{2}}, y^-_{j+\frac{1}{2}}\right) + (1-\alpha_1)(1-\alpha_2)\eta_g\left(x^+_{i+\frac{1}{2}}, y^+_{j+\frac{1}{2}}\right)\end{aligned}$$

represents the weighted average at each corner point of the elements.

- If $\alpha_1 \neq \frac{1}{2}$ and $\alpha_2 = \frac{1}{2}$, the projection error satisfies

$$\int_{K_{ij}} \eta_g v \, \mathrm{d}x \, \mathrm{d}y = 0, \quad \forall\, v \in \mathcal{P}_{k-1}(I_i) \otimes \mathcal{P}_k(J_j), \tag{4.4a}$$

$$\int_{J_j} \{\!\{\eta_g\}\!\}^{\alpha_1,y}_{i+\frac{1}{2},y} v_{i+\frac{1}{2},y} \, \mathrm{d}y = 0, \quad \forall\, v \in \mathcal{P}_k(J_j). \tag{4.4b}$$

- If $\alpha_1 = \frac{1}{2}$ and $\alpha_2 \neq \frac{1}{2}$, the projection error satisfies

$$\int_{K_{ij}} \eta_g v \, \mathrm{d}x \, \mathrm{d}y = 0, \quad \forall\, v \in P_k(I_i) \otimes P_{k-1}(J_j), \tag{4.5a}$$

$$\int_{I_i} \{\!\{\eta_g\}\!\}^{x,\alpha_2}_{x,j+\frac{1}{2}} v_{x,j+\frac{1}{2}} \, \mathrm{d}x = 0, \quad \forall\, v \in P_k(I_i). \tag{4.5b}$$

- If $\alpha_1 = \alpha_2 = \frac{1}{2}$, define $\mathbb{Q}^{1/2,1/2} g$ as the local L^2-projection. Namely, the projection error satisfies

$$\iint_{K_{ij}} \eta_g v \, \mathrm{d}x \, \mathrm{d}y = 0, \quad \forall\, v \in \mathcal{P}_k(I_i) \otimes \mathcal{P}_k(J_j). \tag{4.6}$$

Here and below, the element indexes are taken from $i = 1, 2, \ldots, N_x$ and $j = 1, 2, \ldots, N_y$. For more details about GGR projections, please refer to [4].

Lemma 4.1 *Let g be a smooth function. There exists a bounding constant $C > 0$, independent of h and g, such that*

$$\|\eta_g\| + h^{\frac{1}{2}} \|\eta_g\|_{\Gamma_h} \le C \|g\|_{k+1} h^{k+1}. \tag{4.7}$$

Here and below, $\|g\|_{k+1}$ is the standard norm of g in the Sobolev space $H^{k+1}(\Omega)$.

The purpose of GGR projection is simultaneously eliminating the projection error both in the interior of each element and at the boundary point of each element. In one-dimensional case, this purpose can be totally implemented. Although this purpose can not be able to explicitly achieved in the multi-dimensional space, there fortunately holds the following super-convergence property to guarantee the sharp error estimate.

Lemma 4.2 *Let g be a smooth function. If both $\alpha_1 \neq 1/2$ and $\alpha_2 \neq 1/2$, there holds*

$$\mathcal{H}_{\kappa}^{\alpha_\kappa}(\eta_g, v) \leq Ch^{k+1}\|g\|_{k+2}\|v\|, \quad \forall\, v \in V_h, \tag{4.8}$$

If one parameter $\alpha_\kappa \neq 1/2$ and the other parameter is equal to $1/2$, there holds

$$\mathcal{H}_{\kappa}^{\alpha_\kappa}(\eta_g, v) = 0, \quad \forall\, v \in V_h. \tag{4.9}$$

The super-convergence property (4.8) has been discussed in [4]. The identity (4.9) is implied by the definition of GGR projection, which is mainly used for the auxiliary variables.

Remark 4.1 If $\alpha_1 = \alpha_2 = 1/2$, the super-convergence property (4.8) holds only when the partition is uniform and the degree k is even. In this paper we do not care about this case.

4.2 Modified GGR Projection

If the parameters used in numerical fluxes in each space direction are not the same, the sharp error estimate can not be achieved by directly using the above GGR projections to each variable. Motivated by the idea in [4], we introduce the modified GGR projection for any vector-valued functions, which is defined in a coupled form as follows.

Let $\boldsymbol{\alpha} = (\alpha_1, \alpha_2, \alpha_3, \alpha_4)$ and $\boldsymbol{\beta} = (\beta_1, \beta_2, \beta_3, \beta_4)$ be arbitrary parameter vectors. For simplicity, assume below that every components in $\boldsymbol{\alpha}$ are not equal to $1/2$. For any smooth function $\boldsymbol{v} = (g, g_1, g_2, g_3, g_4)$, the modified GGR projection is defined as

$$\mathbb{W}^{\boldsymbol{\alpha},\boldsymbol{\beta}}\boldsymbol{v} = \left(\mathbb{Q}^{\alpha_1,\alpha_2} g,\ \mathbb{X}^{\alpha_3,\beta_1} g_1,\ \mathbb{Y}^{\alpha_4,\beta_2} g_2,\ \mathbb{X}^{\alpha_3,\beta_3} g_3,\ \mathbb{Y}^{\alpha_4,\beta_4} g_4\right) \in (V_h)^5. \tag{4.10}$$

The first component has been defined in (4.3), and the last four components have taken account on the projection error of the first component on element boundary. To show that, denote the projection error by $\boldsymbol{v} - \mathbb{W}^{\boldsymbol{\alpha},\boldsymbol{\beta}}\boldsymbol{v} = (\eta_g, \eta_1, \eta_2, \eta_3, \eta_4)$. For $s = 1$ and $s = 3$, define $\mathbb{X}^{\alpha_3,\beta_s} g_s$ as the unique element in V_h, such that

$$\iint_{K_{ij}} \eta_s v \,\mathrm{d}x\,\mathrm{d}y = 0, \quad \forall\, v \in \mathcal{P}_{k-1}(I_i) \otimes \mathcal{P}_k(J_j), \tag{4.11a}$$

$$\int_{J_j} \{\!\{\eta_s\}\!\}_{i+\frac{1}{2},y}^{\alpha_3,y} v_{i+\frac{1}{2},y} \,\mathrm{d}y = \beta_s \int_{J_j} [\![\eta_g]\!]_{i+\frac{1}{2},y} v_{i+\frac{1}{2},y} \,\mathrm{d}y, \quad \forall\, v \in \mathcal{P}_k(J_j). \tag{4.11b}$$

Similarly, for $s = 2$ and $s = 4$, define $\mathbb{Y}^{\alpha_4,\beta_s} g_s$ as the unique element in V_h, such that

$$\iint_{K_{ij}} \eta_s v \,\mathrm{d}x\,\mathrm{d}y = 0, \quad \forall\, v \in \mathcal{P}_k(I_i) \otimes \mathcal{P}_{k-1}(J_j), \tag{4.12a}$$

$$\int_{I_i} \{\!\{\eta_s\}\!\}_{x,j+\frac{1}{2}}^{x,\alpha_4} v_{x,j+\frac{1}{2}} \,\mathrm{d}x = \beta_s \int_{I_i} [\![\eta_g]\!]_{x,j+\frac{1}{2}} v_{x,j+\frac{1}{2}} \,\mathrm{d}x, \quad \forall\, v \in \mathcal{P}_k(I_i). \tag{4.12b}$$

When $\beta_s = 0$, they obviously degenerate into the original GGR projections, namely,

$$\mathbb{X}^{\alpha_3,0} g_s = \mathbb{Q}^{\alpha_3,1/2} g_s, \ s = 1, 3; \quad \mathbb{Y}^{\alpha_4,0} g_s = \mathbb{Q}^{1/2,\alpha_4} g_s, \ s = 2, 4.$$

Obviously, $\mathbb{W}^{\boldsymbol{\alpha},\boldsymbol{\beta}}$ is a vector-valued projection operator. By a matrix correction analysis together with the standard L^2-projection [4], we can prove that $\mathbb{W}^{\boldsymbol{\alpha},\boldsymbol{\beta}}\boldsymbol{v}$ uniquely exists and satisfies the following lemma.

Lemma 4.3 *If $\boldsymbol{v} = (g, g_1, g_2, g_3, g_4) \in [H^{k+1}(\Omega)]^5$, we have*

$$\|\eta_g\| + h^{\frac{1}{2}}\|\eta_g\|_{\Gamma_h} \le C\|g\|_{k+1}h^{k+1}, \quad \|\eta_s\| + h^{\frac{1}{2}}\|\eta_s\|_{\Gamma_h} \le C\|\boldsymbol{v}\|_{k+1}(1+\beta_s)h^{k+1}, \tag{4.13}$$

for $s = 1, 2, 3, 4$. Here and below the bounding constant $C > 0$ is also independent of $\boldsymbol{\beta}$, and

$$\|\boldsymbol{v}\|_{k+1} = \left(\|g\|_{k+1}^2 + \sum_{s=1}^{4}\|g_s\|_{k+1}^2\right)^{1/2}.$$

Since the proof is very similar as that in [4], the detailed process is omitted.

4.3 Proof of Theorem 4.1

Associated with the exact solution $\boldsymbol{Z} = (U, Q_1, Q_2, W, P_1, P_2)$, of problem (1.1), we introduce the reference function $\boldsymbol{Z}_h = (U_h, Q_{1h}, Q_{2h}, W_h, P_{1h}, P_{2h})$, where each component belongs to V_h at any time. In specific, it reads

$$(U_h, Q_{1h}, Q_{2h}, P_{1h}, P_{2h}) = \mathbb{W}^{\boldsymbol{\alpha},\boldsymbol{\beta}}(U, Q_1, Q_2, P_1, P_2), \quad W_h = \mathbb{Q}^{\theta_1,\theta_2}W, \tag{4.14}$$

with $\boldsymbol{\alpha} = (\alpha_1, \alpha_2, 1-\theta_1, 1-\theta_2)$ and $\boldsymbol{\beta} = (\beta_1, \beta_2, \beta_3, \beta_4)$. Here the parameters θ_1 and θ_2 are those used in the numerical fluxes, and the other parameters will be determined later.

Denote the numerical error by $\boldsymbol{e} = \boldsymbol{z} - \boldsymbol{Z}$. As usual, there holds the decomposition $\boldsymbol{e} = \boldsymbol{\xi} - \boldsymbol{\eta}$, where $\boldsymbol{\xi} = \boldsymbol{z} - \boldsymbol{Z}_h = (\boldsymbol{\xi}_{uq}, \boldsymbol{\xi}_{wp})$ is the error's projection and $\boldsymbol{\eta} = \boldsymbol{Z} - \boldsymbol{Z}_h = (\boldsymbol{\eta}_{uq}, \boldsymbol{\eta}_{wp})$ is the projection error. By Lemmas 4.1 and 4.3, we have

$$\|\eta_g\| + \|(\eta_g)_t\| + h^{\frac{1}{2}}\|\eta_g\|_{\Gamma_h} \le CAh^{k+1}, \qquad g = u, w, \tag{4.15a}$$

$$\|\eta_{q_\kappa}\| + \|(\eta_{q_\kappa})_t\| + h^{\frac{1}{2}}\|\eta_{q_\kappa}\|_{\Gamma_h} \le CA(1+\beta_\kappa)h^{k+1}, \tag{4.15b}$$

$$\|\eta_{p_\kappa}\| + \|(\eta_{p_\kappa})_t\| + h^{\frac{1}{2}}\|\eta_{p_\kappa}\|_{\Gamma_h} \le CA(1+\beta_{\kappa+2})h^{k+1}, \tag{4.15c}$$

since both the original GGR projection and the modified GGR projection are linear and defined independent of the time.

Owing to the triangle inequality, the remaining work is to sharply estimate $\boldsymbol{\xi}$. To that purpose, we set up the error equations about this variable. Due to the imbedding theorem in Sobolev space, the exact solution at any time is continuous in space. Since the numerical fluxes are consistence, we can easily achieve for $t \in (0, T]$,

$$\left\langle(\boldsymbol{\xi}_{uq})_t, \boldsymbol{v}_{uq}\right\rangle = \left\langle\boldsymbol{\xi}_{wp}, \boldsymbol{v}_{uq}\right\rangle + \left\langle\widetilde{\boldsymbol{\Psi}_{uq}}, \boldsymbol{v}_{uq}\right\rangle, \quad \left\langle\boldsymbol{\xi}_{wp}, \boldsymbol{v}_{wp}\right\rangle = \mathcal{H}(\boldsymbol{\xi}, \boldsymbol{v}_{wp}) + \left\langle\widetilde{\boldsymbol{\Psi}_{wp}}, \boldsymbol{v}_{wp}\right\rangle, \tag{4.16}$$

for any test functions $\boldsymbol{v}_{uq}$ and $\boldsymbol{v}_{wp} \in (V_h)^3$. The formulations have the same construct as that in (2.13). Here $\widetilde{\boldsymbol{\Psi}_{uq}}$ and $\widetilde{\boldsymbol{\Psi}_{wp}} \in (V_h)^3$ depend on the projection errors, satisfying respectively

$$\left\langle\widetilde{\boldsymbol{\Psi}_{uq}}, \boldsymbol{v}_{uq}\right\rangle = \left\langle(\boldsymbol{\eta}_{uq})_t, \boldsymbol{v}_{uq}\right\rangle - \left\langle\boldsymbol{\eta}_{wp}, \boldsymbol{v}_{uq}\right\rangle, \ \forall\, \boldsymbol{v}_{uq} \in (V_h)^3, \tag{4.17a}$$

$$\left\langle\widetilde{\boldsymbol{\Psi}_{wp}}, \boldsymbol{v}_{wp}\right\rangle = \left\langle\boldsymbol{\eta}_{wp}, \boldsymbol{v}_{wp}\right\rangle - \mathcal{H}(\boldsymbol{\eta}, \boldsymbol{v}_{wp}), \ \forall\, \boldsymbol{v}_{wp} \in (V_h)^3. \tag{4.17b}$$

By (3.5a) and (4.17), we can define $\widetilde{Y}_\kappa \in V_h$ such that

$$\left(\widetilde{Y}_\kappa, v\right) = \left((\eta_{q_\kappa})_t, v\right) + \mathcal{H}_\kappa^{\theta_\kappa}((\eta_u)_t, v), \ \forall\, v \in V_h. \tag{4.18}$$

For both LDG schemes, we can respectively find out the unique element $\widetilde{S}_\kappa(0) \in V_h$, such that

$$\left(\xi_{q_\kappa}(0), v\right) + \mathcal{H}_\kappa^{\theta_\kappa}(\xi_u(0), v) = \left(\widetilde{S}_\kappa(0), v\right), \quad \forall\, v \in V_h, \tag{4.19}$$

where $\xi_u(0) = \mathbb{Q}^{\theta_1,\theta_2}U(0) - \mathbb{Q}^{\alpha_1,\alpha_2}U(0)$. Furthermore, we have

1. The LDG(I) scheme. Since $q_\kappa(0)$ is defined by (2.12a), there holds

$$\begin{aligned}\left(\widetilde{S}_\kappa(0), v\right) &= \left(\eta_{q_\kappa}(0), v\right) + \mathcal{H}_\kappa^{\theta_\kappa}(\xi_u(0), v)\\ &= \left(\eta_{q_\kappa}(0), v\right) + \mathcal{H}_\kappa^{\theta_\kappa}(\eta_u(0), v) + \mathcal{H}_\kappa^{\theta_\kappa}(e_u(0), v), \quad \forall v \in V_h,\end{aligned} \tag{4.20a}$$

where $e_u(0) = \mathbb{Q}^{\theta_1,\theta_2}U(0) - U(0)$. Together with (4.18), we can follow (3.5b) and define $\widetilde{\Phi}_\kappa \in V_h$ such that

$$\begin{aligned}\left(\widetilde{\Phi}_\kappa, v\right) &= \left(\int_0^t \widetilde{Y}_\kappa(s)\mathrm{d}s + \widetilde{S}_\kappa(0), v\right)\\ &= \left(\eta_{q_\kappa}, v\right) + \mathcal{H}_\kappa^{\theta_\kappa}(\eta_u, v) + \mathcal{H}_\kappa^{\theta_\kappa}(e_u(0), v), \quad \forall\, v \in V_h.\end{aligned} \tag{4.20b}$$

2. The LDG(II) scheme. Since $q_\kappa(0)$ is defined by (2.12b), there holds

$$\left(\widetilde{S}_\kappa(0), v\right) = \left(\eta_{q_\kappa}(0), v\right) + \mathcal{H}_\kappa^{\theta_\kappa}(\eta_u(0), v), \quad \forall\, v \in V_h. \tag{4.21a}$$

Similarly, we have

$$\left(\widetilde{\Phi}_\kappa, v\right) = \left(\eta_{q_\kappa}, v\right) + \mathcal{H}_\kappa^{\theta_\kappa}(\eta_u, v), \ \forall\, v \in V_h. \tag{4.21b}$$

It is easy to see that the initial error causes a more affection in the LDG(I) scheme.

Now we are ready to estimate the error's projection $\boldsymbol{\xi}$ by using Lemma 3.5. To that end, we have to separately bound $\widetilde{\boldsymbol{\Psi}_{uq}}$, $\widetilde{\boldsymbol{\Psi}_{wp}}$, $\widetilde{Y}_\kappa$, $\widetilde{\Phi}_\kappa$, and $\|\boldsymbol{\xi}_{uq}(0)\|_\mu$. For simplicity, below we assume those parameters in the modified GGR projection satisfies

$$\varepsilon\beta_\kappa + \mu\beta_{\kappa+2} = c_\kappa(\alpha_\kappa - \gamma_\kappa). \tag{4.22}$$

Below the related estimates are given one by one.

- Taking $\boldsymbol{v}_{uq} = \widetilde{\boldsymbol{\Psi}_{uq}}$ in (4.17a), and using Cauchy–Schwarz inequality, we have

$$\|\widetilde{\boldsymbol{\Psi}_{uq}}\|_\mu \le \|(\boldsymbol{\eta}_{uq})_t\|_\mu + \|\boldsymbol{\eta}_{wp}\|_\mu \le CA[1 + \sqrt{\mu}(\beta_1 + \beta_2 + \beta_3 + \beta_4)]h^{k+1}, \tag{4.23}$$

where the approximation property (4.15) is used.

- Taking $\boldsymbol{v}_{wp} = \widetilde{\boldsymbol{\Psi}_{wp}}$ in (4.17b) and noticing the definition of the modified GGR projection, after some manipulations we get

$$\|\widetilde{\boldsymbol{\Psi}_{wp}}\|_\mu^2 = \left\langle \boldsymbol{\eta}_{wp}, \widetilde{\boldsymbol{\Psi}_{wp}}\right\rangle + \sum_{\kappa=1}^{2}\left[\mu\mathcal{H}_\kappa^{\theta_\kappa}(\eta_w, \widetilde{\Psi_{p_\kappa}}) - c_\kappa\mathcal{H}_\kappa^{\alpha_\kappa}(\eta_u, \widetilde{\Psi_w})\right].$$

Using Cauchy–Schwarz inequality, the approximation property (4.15), and the superconvergence property (Lemma 4.2), we have

$$\|\widetilde{\boldsymbol{\Psi}_{wp}}\|_\mu \le CA[1 + \sqrt{\mu}(\beta_3 + \beta_4)]h^{k+1}. \tag{4.24}$$

- Taking $v = \widetilde{Y}_\kappa$ in (4.18), and noticing the simple fact that

$$\mathcal{H}_\kappa^{\theta_\kappa}((\eta_u)_t, \widetilde{Y}_\kappa) - \mathcal{H}_\kappa^{\alpha_\kappa}((\eta_u)_t, \widetilde{Y}_\kappa) = (\alpha_\kappa - \theta_\kappa)\Big([\![(\eta_u)_t]\!], [\![\widetilde{Y}_\kappa]\!]\Big)_{\Gamma_h^\kappa},$$

  we can have, from the approximation property (4.15) and the inverse inequality (3.3), that

$$\|\widetilde{Y}_\kappa\| \le CA[1 + \beta_\kappa + h^{-1}|\alpha_\kappa - \theta_\kappa|]h^{k+1}. \tag{4.25}$$

- Since $u(0)$ is given by (2.11) for both LDG schemes, it is followed from Lemma 4.1 that $\|\xi_u(0)\| \le CAh^{k+1}$ and $\|\eta_u(0)\| \le CAh^{k+1}$. Actually, there holds $\xi_u(0) = 0$ if $\alpha_\kappa = \theta_\kappa$. No matter whether $q_\kappa(0)$ is given by (2.12a) or (2.12b), there always holds

$$\|\eta_{q_\kappa}(0)\| \le CA(1 + \beta_\kappa)h^{k+1}, \tag{4.26a}$$

$$\|\xi_{q_\kappa}(0)\| \le CA(1 + \beta_\kappa)h^{k+1}, \tag{4.26b}$$

$$\|\widetilde{S}_\kappa(0)\| \le CA[1 + \beta_\kappa + h^{-1}|\alpha_\kappa - \theta_\kappa|]h^{k+1}. \tag{4.26c}$$

The first inequality is obtained directly from (4.15). However, the analysis to the second one looks a little different.

1. The LDG(I) scheme. Since $q_\kappa(0)$ is defined by (2.12a), we can get (4.26b) by using the triangle inequality and the approximation property of the local L^2-projection.
2. The LDG(II) scheme: Since $q_\kappa(0)$ is defined by (2.12b), we can have (4.26b) by taking $v = \xi_{q_\kappa}(0)$ in the equivalent expression of (4.19) with (4.21a), namely

$$\Big(\xi_{q_\kappa}(0), v\Big) = \Big(\eta_{q_\kappa}(0), v\Big) - \mathcal{H}_\kappa^{\theta_\kappa}(e_u(0), v), \ \forall\, v \in V_h.$$

   Here we have used respectively the approximation property (4.15) and Lemma 4.2 to bound the right-hand side.

The last one is obtained by the approximation property (4.15) and super-convergence property (Lemma 4.2) of GGR projection. Here the last term is resulted from the difference between the parameters used in the DG discretization.

- Noticing (4.26c), after a similar discussion as above, we can bound $\widetilde{\Phi}_\kappa$ in the form

$$\|\widetilde{\Phi}_\kappa\| \le CA[1 + \beta_\kappa + h^{-1}|\alpha_\kappa - \theta_\kappa|]h^{k+1}, \tag{4.27}$$

  which holds for both LDG schemes.

Below we choose some different values for those parameters in the modified GGR projection. Three groups of parameters are considered, which all satisfy the relationship (4.22). The parameters and the corresponding estimates are listed in Table 1.

Collecting up the above estimates and using Lemma 3.5. we induce from the error equations that

$$\|\boldsymbol{\xi}_{uq}\|_\mu \le CA(1 + T)\Big[h^{k+1} + \varrho h^k\Big], \quad \forall\, t \in [0, T], \tag{4.28}$$

where the bounding constant $C > 0$ is independent of h, ε^{-1}, μ^{-1} and T. Note that the notation ϱ has been defined in (4.2). Finally, by using the triangle inequality and approximation property (4.15) again, we can complete the proof of Theorem 4.1.

Table 1 Estimates for three groups of parameters. The factor CAh^{k+1} is omitted, and $\delta_\kappa = \theta_\kappa - \gamma_\kappa$

	$\alpha_\kappa = \theta_\kappa$, $\beta_\kappa = \varepsilon^{-1} c_\kappa \delta_\kappa$, $\beta_{2+\kappa} = 0$.	$\alpha_\kappa = \theta_\kappa$, $\beta_\kappa = 0$, $\beta_{2+\kappa} = \mu^{-1} c_\kappa \delta_\kappa$.	$\alpha_\kappa = \gamma_\kappa$, $\beta_\kappa = 0$, $\beta_{2+\kappa} = 0$.
$\Vert\widetilde{\boldsymbol{\Psi}_{uq}}\Vert_\mu$	$1 + \sum_{\kappa=1}^{2} \frac{c_\kappa \sqrt{\mu}}{\varepsilon} \lvert\delta_\kappa\rvert$	$1 + \sum_{\kappa=1}^{2} \frac{c_\kappa}{\sqrt{\mu}} \lvert\delta_\kappa\rvert$	1
$\Vert\widetilde{\boldsymbol{\Psi}_{wp}}\Vert_\mu$	1	$1 + \sum_{\kappa=1}^{2} \frac{c_\kappa}{\sqrt{\mu}} \lvert\delta_\kappa\rvert$	1
$\Vert\widetilde{Y_\kappa}\Vert$	$1 + \frac{c_\kappa}{\varepsilon} \lvert\delta_\kappa\rvert$	1	$1 + h^{-1} \lvert\delta_\kappa\rvert$
$\Vert\widetilde{\Phi_\kappa}\Vert$	$1 + \frac{c_\kappa}{\varepsilon} \lvert\delta_\kappa\rvert$	1	$1 + h^{-1} \lvert\delta_\kappa\rvert$
$\Vert\boldsymbol{\xi}_{uq}(0)\Vert_\mu$	$1 + \sum_{\kappa=1}^{2} \frac{c_\kappa \sqrt{\mu}}{\varepsilon} \lvert\delta_\kappa\rvert$	1	1

5 Extension to Fully-Discrete LDG Scheme

In this section, we employ the third-order explicit TVDRK time-marching and present a fully-discrete LDG scheme for (1.1). In what follows, we use ℓ to represent the stage index, which is always taken from $\{0, 1, 2\}$. When $\ell = 0$, it may be omitted.

5.1 Fully-Discrete LDG Scheme

Denote by $\{t^n = n\tau\}_{n=0,1,\ldots,N_t}$ the uniform subdivision of the time interval $[0, T]$, with the time step $\tau = T/N_t$. Here N_t is an arbitrary positive integer. The time step could actually change from step to step, but in this paper it is taken as a constant for simplicity.

To save space, we present here the fully-discrete LDG scheme for (2.13). Suppose that the numerical solution at the current time t^n, denoted by $z^n = z^{n,0} \in (V_h)^6$, has been available, the numerical solution at the next time t^{n+1}, denoted by $z^{n+1} = z^{n,3} \in (V_h)^6$, can be sought through two intermediate solutions $z^{n,1} \in (V_h)^6$ and $z^{n,2} \in (V_h)^6$, such that

$$\left\langle z_{uq}^{n,1}, \boldsymbol{v}_{uq} \right\rangle = \left\langle z_{uq}^{n}, \boldsymbol{v}_{uq} \right\rangle + \tau \left\langle z_{wp}^{n} + \boldsymbol{\Psi}_{uq}^{n}, \boldsymbol{v}_{uq} \right\rangle, \tag{5.1a}$$

$$\left\langle z_{uq}^{n,2}, \boldsymbol{v}_{uq} \right\rangle = \frac{3}{4}\left\langle z_{uq}^{n}, \boldsymbol{v}_{uq} \right\rangle + \frac{1}{4}\left\langle z_{uq}^{n,1}, \boldsymbol{v}_{uq} \right\rangle + \frac{\tau}{4}\left\langle z_{wp}^{n,1} + \boldsymbol{\Psi}_{uq}^{n,1}, \boldsymbol{v}_{uq} \right\rangle, \tag{5.1b}$$

$$\left\langle z_{uq}^{n+1}, \boldsymbol{v}_{uq} \right\rangle = \frac{1}{3}\left\langle z_{uq}^{n}, \boldsymbol{v}_{uq} \right\rangle + \frac{2}{3}\left\langle z_{uq}^{n,2}, \boldsymbol{v}_{uq} \right\rangle + \frac{2\tau}{3}\left\langle z_{wp}^{n,2} + \boldsymbol{\Psi}_{uq}^{n,2}, \boldsymbol{v}_{uq} \right\rangle, \tag{5.1c}$$

as well as

$$\left\langle z_{wp}^{n,\ell}, \boldsymbol{v}_{wp} \right\rangle = \mathcal{H}(z^{n,\ell}, \boldsymbol{v}_{wp}) + \left\langle \boldsymbol{\Psi}_{wp}^{n,\ell}, \boldsymbol{v}_{wp} \right\rangle, \quad \ell = 0, 1, 2, \tag{5.1d}$$

hold for any test functions $\boldsymbol{v}_{uq} \in (V_h)^3$ and $\boldsymbol{v}_{wp} \in (V_h)^3$.

The initial solutions are defined in the same way, namely $z_{uq}^0 = z_{uq}(0)$, where $z_{uq}(0)$ is given by (2.11) and (2.12). Similarly as (2.16), we can also assume a general relationship

$$\left(q_\kappa^0, v\right) + \mathcal{H}_\kappa^{\theta_\kappa}(u^0, v) = \left(S_\kappa^0, v\right), \quad \forall\, v \in V_h, \tag{5.2}$$

for the initial solutions, where $S_\kappa^0 = S_\kappa(0)$. This completes the definition of fully-discrete LDG scheme.

Let $\boldsymbol{\Psi}_{uq}^{n,\ell} = \boldsymbol{\Psi}_{wp}^{n,\ell} = 0$, then the above formulations give the fully-discrete LDG scheme of (1.1). Similar as the semi-discrete case, the schemes with two types of initial solution are called the fully-discrete LDG(I) scheme and LDG(II) scheme, respectively.

Remark 5.1 With the fully-discrete LDG scheme of problem (1.1), we are ready to show the numerical advantages contributed from the formulation (2.8a). They are twofold.

1. Since both the stage solutions and the test functions belong to the same finite element space, the time-marching process, from (5.1a) to (5.1c), is equivalent to directly adopting the same action to every freedom of stage solutions. Hence the efficiency of solution's updating is greatly improved.
2. As soon as the numerical solution $z_{uq}^{n,\ell}$ is obtained, the numerical solution $z_{wp}^{n,\ell}$ at the same stage time will be resolved out by using (5.1d). This is a simple application of the LDG method to the elliptic problem. Those existing LDG routines can be employed in the numerical computation.

In the next two subsections, we would like to present the stability and error estimates. Since the proof is similar as that in the previous sections and in [14,23], we just present the snapshot of proof and point out the important points.

5.2 Stability Analysis

In addition to the definition (3.5), we define

$$Y_\kappa^{n,\ell} = \Psi_{p_\kappa}^{n,\ell} + \Psi_{q_\kappa}^{n,\ell} + \mathcal{H}_\kappa^{\theta_\kappa}\Psi_u^{n,\ell}, \tag{5.3a}$$

for any $n \geq 0$ and $\ell \in \{0, 1, 2\}$. Let $\Phi_\kappa^0 = S_\kappa^0$, and recursively define

$$\begin{aligned} \Phi_\kappa^{n,1} = \Phi_\kappa^n + Y_\kappa^n\tau, \quad \Phi_\kappa^{n,2} &= \Phi_\kappa^n + \frac{\tau}{4}(Y_\kappa^n + Y_\kappa^{n,1}), \\ \Phi_\kappa^{n+1} &= \Phi_\kappa^n + \frac{\tau}{6}(Y_\kappa^n + Y_\kappa^{n,1} + 4Y_\kappa^{n,2}), \end{aligned} \tag{5.3b}$$

which can be looked upon as the approximations of (3.5b) at different stage time.

Some linear combinations of (5.1) yield the following lemma, almost the same as Lemma 3.4. The proof is trivial, so omitted to save space.

Lemma 5.1 *The numerical solution of (5.1) satisfies*

$$\left(q_\kappa^{n,\ell}, v\right) + \mathcal{H}_\kappa^{\theta_\kappa}(u^{n,\ell}, v) = \left(\Phi_\kappa^{n,\ell}, v\right), \quad \forall\, v \in V_h. \tag{5.4}$$

Following [23,24], we introduce for the stage functions $\{g^{n,\ell}\}$ three types of difference

$$\mathbb{D}_1 g^n = g^{n,1} - g^n, \quad \mathbb{D}_2 g^n = 2g^{n,2} - g^{n,1} - g^n, \quad \mathbb{D}_3 g^n = g^{n+1} - 2g^{n,2} + g^n. \tag{5.5}$$

In some sense, they can be understood as the approximation of the time derivatives from the first order to the third order [24]. For simplicity of notations, we define $\mathbb{D}_0 g^n = g^n$. Note that these definitions can be extended to the vector-valued functions.

The following relationship plays an important role in the next analysis. The detailed proof will be given in the "Appendix".

Lemma 5.2 *Denote $\lambda_c = c\tau h^{-1}$ and $\lambda_d = \varepsilon\tau h^{-2}$, where $c = \sqrt{c_1^2 + c_2^2}$. For $\ell = 0, 1, 2$, the solution of (5.1) satisfies*

$$\|\mathbb{D}_{\ell+1} z_{uq}^n\|_\mu^2 \leq b_\ell M^2\Big[\lambda_c^2\|\mathbb{D}_\ell z_{uq}^n\|_\mu^2 + \varepsilon\lambda_d\|\mathbb{D}_\ell \boldsymbol{q}^n\|^2\tau\Big] + C\Big[\|\mathbb{D}_\ell \boldsymbol{\Psi}_{uq}^n\|_\mu^2 + \|\mathbb{D}_\ell \boldsymbol{\Psi}_{wp}^n\|_\mu^2\Big]\tau^2, \tag{5.6}$$

where $b_0 = 16, b_1 = 4$, and $b_2 = 2$. Here the positive constant M has been given in Lemma 3.3, and the bounding constant $C > 0$ is independent of $n, h, \tau, \varepsilon^{-1}, \mu^{-1}$ and T.

To carry out the stability analysis, we take three test functions in the LDG scheme, namely, $\boldsymbol{v}_{uq} = \boldsymbol{z}_{uq}^{n}$ in (5.1a), $\boldsymbol{v}_{uq} = 4\boldsymbol{z}_{uq}^{n,1}$ in (5.1b), and $\boldsymbol{v}_{uq} = 6\boldsymbol{z}_{uq}^{n,2}$ in (5.1c). Summing up the resulted equations, after some manipulations we can get

$$3\|\boldsymbol{z}_{uq}^{n+1}\|_{\mu}^{2} - 3\|\boldsymbol{z}_{uq}^{n}\|_{\mu}^{2} = -\|\mathbb{D}_2\boldsymbol{z}_{uq}^{n}\|_{\mu}^{2} + \mathcal{R}_1^n + \mathcal{R}_2^n + \mathcal{R}_3^n, \tag{5.7}$$

where $d_0 = d_1 = 1$, $d_2 = 4$, and

$$\mathcal{R}_1^n = \sum_{\ell=0}^{2} d_\ell \left\langle \boldsymbol{z}_{wp}^{n,\ell} + \boldsymbol{\Psi}_{uq}^{n,\ell}, \boldsymbol{z}_{uq}^{n,\ell} \right\rangle \tau, \tag{5.8a}$$

$$\mathcal{R}_2^n = 2\left\langle \mathbb{D}_2\boldsymbol{z}_{uq}^{n}, \mathbb{D}_2\boldsymbol{z}_{uq}^{n} \right\rangle + 3\left\langle \mathbb{D}_3\boldsymbol{z}_{uq}^{n}, \mathbb{D}_1\boldsymbol{z}_{uq}^{n} \right\rangle, \tag{5.8b}$$

$$\mathcal{R}_3^n = 3\left\langle \mathbb{D}_3\boldsymbol{z}_{uq}^{n}, \mathbb{D}_2\boldsymbol{z}_{uq}^{n} \right\rangle + 3\left\langle \mathbb{D}_3\boldsymbol{z}_{uq}^{n}, \mathbb{D}_3\boldsymbol{z}_{uq}^{n} \right\rangle. \tag{5.8c}$$

The first term on the right-hand side of (5.7) explicitly shows the additional stability mechanism provided by the third-order explicit TVDRK time-marching. In what follows we are going to separately estimate the above three terms, whose detailed proofs are given in the "Appendix".

Almost the same as that in the semi-discrete case, we can easily achieve that

$$\mathcal{R}_1^n = -\mathcal{S}_{\mathrm{c}}^n - \mathcal{S}_{\mathrm{d}}^n + \Theta_1^n\tau, \tag{5.9a}$$

where two nonnegative terms

$$\mathcal{S}_{\mathrm{c}}^n = \frac{1}{2}\sum_{\ell=0}^{2}\sum_{\kappa=1}^{2} d_\ell c_\kappa(2\gamma_\kappa - 1)\|[\![u^{n,\ell}]\!]\|_{\Gamma_h^\kappa}^2\tau, \quad \mathcal{S}_{\mathrm{d}}^n = \sum_{\ell=0}^{2} d_\ell\varepsilon\|\boldsymbol{q}^{n,\ell}\|^2\tau, \tag{5.9b}$$

represent the stability mechanism in each step of time-marching, and

$$\Theta_1^n = \sum_{\ell=0}^{2}\sum_{\kappa=1}^{2} d_\ell\left(\Phi_\kappa^{n,\ell}, \varepsilon q_\kappa^{n,\ell} + \mu p_\kappa^{n,\ell}\right) + \sum_{\ell=0}^{2} d_\ell\left(\Psi_w^{n,\ell}, u^{n,\ell}\right) + \sum_{\ell=0}^{2} d_\ell\left\langle \boldsymbol{\Psi}_{uq}^{n,\ell}, \boldsymbol{z}_{uq}^{n,\ell}\right\rangle. \tag{5.9c}$$

The remaining two terms strongly depend on the relationships among differences of stage solutions, which involve the temporal–spatial condition to control the errors resulted from the time-marching. After a little long and technical deduction, we can obtain

$$\mathcal{R}_2^n \le \left[\frac{1}{4} + 8M\lambda_{\mathrm{c}}(\gamma_1+\gamma_2-1)\right]\|\mathbb{D}_2\boldsymbol{z}_{uq}^{n}\|_{\mu}^{2} + \frac{1}{2}\mathcal{S}_{\mathrm{c}}^n + 16M^2\lambda_{\mathrm{d}}\mathcal{S}_{\mathrm{d}}^n + \Theta_{21}^n\tau + \Theta_{22}^n\tau + \Theta_{23}^n\tau, \tag{5.10}$$

where

$$\Theta_{21}^n = \left(\mathbb{D}_1\Psi_w^n, \mathbb{D}_2u^n\right) + \left\langle \mathbb{D}_1\boldsymbol{\Psi}_{uq}^n, \mathbb{D}_2\boldsymbol{z}_{uq}^n\right\rangle + \left(\mathbb{D}_2\Psi_w^n, \mathbb{D}_1u^n\right) + \left\langle \mathbb{D}_2\boldsymbol{\Psi}_{uq}^n, \mathbb{D}_1\boldsymbol{z}_{uq}^n\right\rangle, \tag{5.11a}$$

$$\Theta_{22}^n = \varepsilon\sum_{\kappa=1}^{2}\left[-\left(\mathbb{D}_2\Phi_\kappa^n, \mathbb{D}_1q_\kappa^n\right) + \left(\mathbb{D}_1\Phi_\kappa^n, \mathbb{D}_2q_\kappa^n\right)\right], \tag{5.11b}$$

$$\Theta_{23}^n = \mu\sum_{\kappa=1}^{2}\left[\left(\mathbb{D}_2\Phi_\kappa^n, \mathbb{D}_1p_\kappa^n\right) + \left(\mathbb{D}_1\Phi_\kappa^n, \mathbb{D}_2p_\kappa^n\right)\right]. \tag{5.11c}$$

Let $\Theta_3^n = C\Big[\|\mathbb{D}_2\boldsymbol{\Psi}_{uq}^n\|_\mu^2 + \|\mathbb{D}_2\boldsymbol{\Psi}_{wp}^n\|_\mu^2\Big]\tau$. By Lemma 5.2 and Young's inequality, we have

$$\begin{aligned}\mathcal{R}_3^n &\le 3\|\mathbb{D}_2 z_{uq}^n\|_\mu\|\mathbb{D}_3 z_{uq}^n\|_\mu + 3\|\mathbb{D}_3 z_{uq}^n\|_\mu^2 \le \frac{1}{4}\|\mathbb{D}_2 z_{uq}^n\|_\mu^2 + 12\|\mathbb{D}_3 z_{uq}^n\|_\mu^2\\ &\le \Big[24M^2\lambda_{\mathrm{c}}^2 + \frac{1}{4}\Big]\|\mathbb{D}_2 z_{uq}^n\|_\mu^2 + 72M^2\lambda_{\mathrm{d}}\mathcal{S}_{\mathrm{d}}^n + \Theta_3^n\tau,\end{aligned} \tag{5.12}$$

where the definition of $\mathbb{D}_2\boldsymbol{q}^n$ and Jensen inequality are used.

Collecting up the above conclusions into the energy equation (5.7), we can get

$$3\|z_{uq}^{n+1}\|_\mu^2 - 3\|z_{uq}^n\|_\mu^2 + \frac{1}{2}\mathcal{S}_{\mathrm{c}}^n + \Upsilon_1\|\mathbb{D}_2 z_{uq}^n\|_\mu^2 + \Upsilon_2\mathcal{S}_{\mathrm{d}}^n \le \Theta_1^n\tau + \sum_{j=1}^{3}\Theta_{2j}^n\tau + \Theta_3^n\tau, \tag{5.13}$$

where $\Upsilon_1 = \frac{1}{2} - 8M\lambda_{\mathrm{c}}(\gamma_1+\gamma_2-1) - 24M^2\lambda_{\mathrm{c}}^2$ and $\Upsilon_2 = 1 - 88M^2\lambda_{\mathrm{d}}$. Under suitable temporal–spatial condition, for example,

$$\lambda_{\mathrm{c}} \le \min\Big\{\frac{1}{96M(\gamma_1+\gamma_2-1)}, \frac{1}{12M}\Big\}, \quad \text{and} \quad \lambda_{\mathrm{d}} \le \frac{1}{176M^2}, \tag{5.14}$$

there hold $\Upsilon_1 \ge \frac{1}{4}$ and $\Upsilon_2 \ge \frac{1}{2}$.

The strong stability for the fully-discrete LDG(II) scheme is followed, since $\boldsymbol{\Psi}_{uq}^{n,\ell} = \boldsymbol{\Psi}_{wp}^{n,\ell} = \mathbf{0}$ and $S_\kappa^0 = 0$, which also implies $Y_\kappa^{n,\ell} = \Phi_\kappa^{n,\ell} \equiv 0$.

Theorem 5.1 *Under the temporal–space condition* (5.14)*, the solution of the fully-discrete LDG(II) scheme satisfies*

$$\|z_{uq}^{n+1}\|_\mu \le \|z_{uq}^n\|_\mu, \quad \forall n \ge 0. \tag{5.15}$$

Let us come back to the inequality (5.13) and estimate the right-hand side. Totally speaking, there are three groups of terms, respectively denoted by G_1^n, G_2^n, and G_3^n. The first one are made up of those terms including $\varepsilon q_\kappa^{n,\ell}$. An application of Cauchy–Schwarz inequality and Young's inequality yields

$$G_1^n \le \sum_{\kappa=1}^{2}\sum_{\ell=0}^{2}\varepsilon d_\ell\Big[\frac{1}{4}\|q_\kappa^{n,\ell}\|^2 + C\|\Phi_\kappa^{n,\ell}\|^2\Big]\tau \le \frac{1}{4}\mathcal{S}_{\mathrm{d}}^n + C\varepsilon\sum_{\kappa=1}^{2}\sum_{\ell=0}^{2}\|\Phi_\kappa^{n,\ell}\|^2\tau. \tag{5.16}$$

The second one are made up of those terms including $\mu p_\kappa^{n,\ell}$, explicitly shown in the form

$$G_2^n = \mu\sum_{\kappa=1}^{2}\Big[\sum_{\ell=0}^{2} d_\ell\Big(\Phi_\kappa^{n,\ell}, p_\kappa^{n,\ell}\Big)\tau + \Big(\mathbb{D}_2\Phi_\kappa^n, \mathbb{D}_1 p_\kappa^n\Big)\tau + \Big(\mathbb{D}_1\Phi_\kappa^n, \mathbb{D}_2 p_\kappa^n\Big)\tau\Big].$$

The estimate to the first term in the bracket is important. Noticing (5.1a)–(5.1c), after some manipulations we can obtain that

$$\begin{aligned}\sum_{\ell=0}^{2} d_\ell\Big(\Phi_\kappa^{n,\ell}, p_\kappa^{n,\ell}\Big)\tau &= \sum_{\ell=0}^{2} d_\ell\Big(\Phi_\kappa^{n,\ell}, \mathbb{E}_{\ell+1}q_\kappa^n\Big) - \sum_{\ell=0}^{2} d_\ell\Big(\Phi_\kappa^{n,\ell}, \Psi_{q_\kappa}^{n,\ell}\Big)\tau\\ &= 6\Big(\Phi_\kappa^{n+1}, q_\kappa^{n+1}\Big) - 6\Big(\Phi_\kappa^n, q_\kappa^n\Big) + \sum_{\ell=0}^{3}\Big(\mathbb{E}_\ell^{\mathrm{inv}}\Phi_\kappa^n, q_\kappa^{n,\ell}\Big)\\ &\quad - \sum_{\ell=0}^{2} d_\ell\Big(\Phi_\kappa^{n,\ell}, \Psi_{q_\kappa}^{n,\ell}\Big)\tau,\end{aligned}$$

where

$$\mathbb{E}_1 q_\kappa^n = q_\kappa^{n,1} - q_\kappa^n, \quad \mathbb{E}_2 q_\kappa^n = 4q_\kappa^{n,2} - q_\kappa^{n,1} - 3q_\kappa^n, \quad \mathbb{E}_3 q_\kappa^n = \frac{3}{2} q_\kappa^{n+1} - q_\kappa^{n,2} - \frac{1}{2} q_\kappa^n, \tag{5.17a}$$

represent each stage time-marching, and

$$\mathbb{E}_0^{\text{inv}} \Phi_\kappa^n = 5\Phi_\kappa^n - 3\Phi_\kappa^{n,1} - 2\Phi_\kappa^{n,2}, \qquad \mathbb{E}_1^{\text{inv}} \Phi_\kappa^n = \Phi_\kappa^n - \Phi_\kappa^{n,1}, \tag{5.17b}$$

$$\mathbb{E}_2^{\text{inv}} \Phi_\kappa^n = 4\Phi_\kappa^{n,1} - 4\Phi_\kappa^{n,2}, \qquad \mathbb{E}_3^{\text{inv}} \Phi_\kappa^n = 6\Phi_\kappa^{n,2} - 6\Phi_\kappa^{n+1}, \tag{5.17c}$$

are resulted from the discrete expression of integration by parts in time direction. Note that all terms in (5.17) can be expressed by the linear combination of $\mathbb{D}_\ell$'s series. By using (5.1a)–(5.1c) again, the remaining two terms in G_2^n can be estimated similarly. Hence, we have

$$\begin{aligned} G_2^n \le \mu \sum_{\kappa=1}^{2} \Big[6\Big(\Phi_\kappa^{n+1}, q_\kappa^{n+1}\Big) - 6\Big(\Phi_\kappa^n, q_\kappa^n\Big) \Big] \\ + \mu \sum_{\kappa=1}^{2} \sum_{\ell=0}^{2} \Big[\frac{1}{T} \| q_\kappa^{n,\ell} \|^2 \tau + CT \| \mathbb{D}_{\ell+1} \Phi_\kappa^n \|^2 \tau^{-1} + C \| \Phi_\kappa^{n,\ell} \|^2 \tau + C \| \Psi_{q_\kappa}^{n,\ell} \|^2 \tau \Big], \end{aligned} \tag{5.18}$$

with the help of Cauchy–Schwarz inequality and Young's inequality. The rest in the right-hand side of (5.13) is denote by G_3^n, which can be easily bounded in the form

$$G_3^n \le C \sum_{\ell=0}^{2} \Big[T^{-1} \| z_{uq}^{n,\ell} \|_\mu^2 + T \| \boldsymbol{\Psi}_{uq}^{n,\ell} \|_\mu^2 + T \| \boldsymbol{\Psi}_{wp}^{n,\ell} \|_\mu^2 \Big] \tau. \tag{5.19}$$

Substituting the above inequalities into (5.13), and summing up this estimate over all time level from 0 to any integer $m < N_t$, we can achieve that

$$3 \| z_{uq}^{m+1} \|_\mu^2 + \frac{1}{2} \sum_{n=0}^{m} \mathcal{S}_{\mathrm{c}}^n + \frac{1}{4} \sum_{n=0}^{m} \mathcal{S}_{\mathrm{d}}^n \le CT^{-1} \sum_{n=0}^{m} \sum_{\ell=0}^{2} \| z_{uq}^{n,\ell} \|_\mu^2 \tau + C\Pi_1^m + C\Pi_2^m + \Pi_{12}^m, \tag{5.20}$$

where

$$\Pi_1^m = \sum_{n=0}^{m} \sum_{\ell=0}^{2} \Big[T \| \boldsymbol{\Psi}_{wp}^{n,\ell} \|_\mu^2 + (1+T) \| \boldsymbol{\Psi}_{uq}^{n,\ell} \|_\mu^2 \Big] \tau, \tag{5.21a}$$

$$\Pi_2^m = \sum_{\kappa=1}^{2} \sum_{n=0}^{m} \sum_{\ell=0}^{2} \Big[T\mu \| \mathbb{D}_{\ell+1} \Phi_\kappa^n \|^2 \tau^{-1} + (\varepsilon + \mu) \| \Phi_\kappa^{n,\ell} \|^2 \tau \Big], \tag{5.21b}$$

$$\Pi_{12}^m = 3 \| z_{uq}^0 \|_\mu^2 + 6\mu \sum_{\kappa=1}^{2} \Big(\Phi_\kappa^{m+1}, q_\kappa^{m+1} \Big) - 6\mu \sum_{\kappa=1}^{2} \Big(\Phi_\kappa^0, q_\kappa^0 \Big). \tag{5.21c}$$

Applying Cauchy–Schwarz inequality and Young's inequality to the last two terms in (5.21c), we can get that $\Pi_{12}^m \le \| z_{uq}^{m+1} \|_\mu^2 + C\Pi_3^m$, where

$$\Pi_3^m = \| z_{uq}^0 \|_\mu^2 + \mu \sum_{\kappa=1}^{2} \Big[\| \Phi_\kappa^{m+1} \|^2 + \| \Phi_\kappa^0 \|^2 \Big]. \tag{5.22}$$

Using Lemma 5.2 and triangle inequality, we can bound $\|z_{uq}^{n,\ell}\|_\mu^2$ by those quantities staying at the integer time levels. Finally, we can employ the discrete Gronwall's inequality and achieve the main conclusion in this subsection.

Lemma 5.3 *Under the temporal–space condition (5.14), the solution of fully-discrete LDG scheme (5.1) satisfies the weak stability*

$$\|z_{uq}^{m+1}\|_\mu^2 \leq C\Pi_1^m + C\Pi_2^m + C\Pi_3^m, \quad m < N_t, \tag{5.23}$$

where the bounding constant $C > 0$ is independent of $h, \tau, \varepsilon^{-1}, \mu^{-1}$ and T.

It is also a weak stability as shown in the semi-discrete case, which is enough for us to obtain the sharp error estimate.

5.3 Error Estimate

In this subsection, we set up the sharp error estimate to the fully-discrete LDG scheme of problem (1.1). The conclusion is stated as follows.

Theorem 5.2 *Assume $U \in W^{3,\infty}(H^{k+2}) \cap W^{4,\infty}(H^1)$, whose regularity boundedness is denoted by B. Then there holds*

$$\max_{n\tau\leq T}\left[\|U(t^n) - u^n\|^2 + \mu\|\boldsymbol{Q}(t^n) - \boldsymbol{q}^n\|^2\right]^{1/2} \leq CB(1+T)\Big[h^{k+1} + \varrho h^k + \tau^3\Big], \tag{5.24}$$

under the spatial–temporal condition (5.14), where the bounding constant $C > 0$ is independent of $h, \tau, \varepsilon^{-1}, \mu^{-1}$ and T.

To prove this theorem, we follow [23] and define the reference function $\boldsymbol{Z}^{n,\ell} = (\boldsymbol{Z}_{uq}^{n,\ell}, \boldsymbol{Z}_{wp}^{n,\ell})$ at each stage time. Paralleled to the Runge–Kutta time-marching, let

$$\boldsymbol{Z}_{uq}^n = \boldsymbol{Z}_{uq}(t^n), \quad \boldsymbol{Z}_{uq}^{n,1} = \boldsymbol{Z}_{uq}^n + \boldsymbol{Z}_{wp}^n\tau, \quad \boldsymbol{Z}_{uq}^{n,2} = \frac{3}{4}\boldsymbol{Z}_{uq}^n + \frac{1}{4}\boldsymbol{Z}_{uq}^{n,1} + \frac{1}{4}\boldsymbol{Z}_{wp}^{n,1}\tau, \tag{5.25}$$

where $\boldsymbol{Z}_{wp}^{n,\ell}$ is the unique solution of the following elliptic system

$$W^{n,\ell} - \mu\nabla\cdot\boldsymbol{P}^{n,\ell} = \varepsilon\nabla\cdot\boldsymbol{Q}^{n,\ell} - \boldsymbol{c}\cdot\nabla U^{n,\ell}, \quad \boldsymbol{P}^{n,\ell} - \nabla W^{n,\ell} = 0, \tag{5.26}$$

subject to the periodic boundary condition. Noticing definition (5.25), an application of Taylor's expansion in time yields

$$\boldsymbol{Z}_{uq}^{n+1} = \frac{1}{3}\boldsymbol{Z}_{uq}^n + \frac{2}{3}\boldsymbol{Z}_{uq}^{n,2} + \frac{2\tau}{3}(\boldsymbol{Z}_{wp}^{n,2} + \boldsymbol{\zeta}_{uq}^{n,2}), \tag{5.27}$$

where $\frac{2}{3}\tau\boldsymbol{\zeta}_{uq}^{n,2}$ is the local truncation error in time direction. Obviously there exists a bounding constant $C > 0$ independent of n, such that

$$\|\boldsymbol{\zeta}_{uq}^{n,2}\|_\mu \leq C\tau^3. \tag{5.28}$$

For convenience of notations, we also denote $\boldsymbol{\zeta}_{uq}^n = \boldsymbol{\zeta}_{uq}^{n,1} = \boldsymbol{0}$.

Denote by $\boldsymbol{e}^{n,\ell} = \boldsymbol{z}^{n,\ell} - \boldsymbol{Z}^{n,\ell}$ the numerical error at each stage time. As usual, we have the decomposition $\boldsymbol{e}^{n,\ell} = \boldsymbol{\xi}^{n,\ell} - \boldsymbol{\eta}^{n,\ell}$, where $\boldsymbol{\eta}^{n,\ell} = (\boldsymbol{\eta}_{uq}^{n,\ell}, \boldsymbol{\eta}_{wp}^{n,\ell})$ is the projection error and $\boldsymbol{\xi}^{n,\ell} = (\boldsymbol{\xi}_{uq}^{n,\ell}, \boldsymbol{\xi}_{wp}^{n,\ell}) \in V_h$ is the error's projection.

Since $\boldsymbol{\eta}^{n,\ell}$ can be bounded by the same inequality as (4.15), the remaining work is to sharply estimate $\boldsymbol{\xi}^{n,\ell}$. To that purpose, we set up the error equations. Multiply the test functions $\boldsymbol{v}_{uq}$ and $\boldsymbol{v}_{wp} \in (V_h)^3$ on both sides of (5.25), (5.26) and (5.27), respectively, and then integrate them in space. Subtracting the resulted identities from the fully-discrete LDG scheme gives the following error equations

$$\left\langle \mathbb{E}_{\ell+1}\boldsymbol{\xi}_{uq}^{n}, \boldsymbol{v}_{uq} \right\rangle = \tau\left\langle \boldsymbol{\xi}_{wp}^{n,\ell} + \widetilde{\boldsymbol{\Psi}_{uq}^{n,\ell}}, \boldsymbol{v}_{uq} \right\rangle, \ \forall\, \boldsymbol{v}_{uq} \in (V_h)^3, \tag{5.29a}$$

$$\left\langle \boldsymbol{\xi}_{wp}^{n,\ell}, \boldsymbol{v}_{wp} \right\rangle = \mathcal{H}(\boldsymbol{\xi}^{n,\ell}, \boldsymbol{v}_{wp}) + \left\langle \widetilde{\boldsymbol{\Psi}_{wp}^{n,\ell}}, \boldsymbol{v}_{wp} \right\rangle, \ \forall\, \boldsymbol{v}_{wp} \in (V_h)^3, \tag{5.29b}$$

where both $\widetilde{\boldsymbol{\Psi}_{uq}^{n,\ell}}$ and $\widetilde{\boldsymbol{\Psi}_{wp}^{n,\ell}}$ are given functions in $(V_h)^3$, satisfying respectively

$$\left\langle \widetilde{\boldsymbol{\Psi}_{uq}^{n,\ell}}, \boldsymbol{v}_{uq} \right\rangle = \left\langle \tau^{-1}\mathbb{E}_{\ell+1}\boldsymbol{\eta}_{uq}^{n} - \boldsymbol{\eta}_{wp}^{n,\ell} - \boldsymbol{\zeta}_{uq}^{n,\ell}, \boldsymbol{v}_{uq} \right\rangle, \ \forall\, \boldsymbol{v}_{uq} \in (V_h)^3, \tag{5.30a}$$

$$\left\langle \widetilde{\boldsymbol{\Psi}_{wp}^{n,\ell}}, \boldsymbol{v}_{wp} \right\rangle = \left\langle \boldsymbol{\eta}_{wp}^{n,\ell}, \boldsymbol{v}_{wp} \right\rangle - \mathcal{H}(\boldsymbol{\eta}^{n,\ell}, \boldsymbol{v}_{wp}), \ \forall\, \boldsymbol{v}_{wp} \in (V_h)^3. \tag{5.30b}$$

It follows from (5.3a) and (5.30) that

$$\tau\left(\widetilde{Y_{\kappa}^{n,\ell}}, v\right) = \tau\left(\widetilde{\Psi_{p_\kappa}^{n,\ell}} + \widetilde{\Psi_{q_\kappa}^{n,\ell}} + \mathcal{H}_{\kappa}^{\theta_\kappa}\widetilde{\Psi_{u}^{n,\ell}}, v\right) = \left(\mathbb{E}_{\ell+1}\eta_{q_\kappa}^{n}, v\right) + \mathcal{H}_{\kappa}^{\theta_\kappa}(\mathbb{E}_{\ell+1}\eta_{u}^{n}, v), \tag{5.31}$$

for any $v \in V_h$. Note that we have used in this process the simple fact that $\zeta_{q_\kappa}^{n,\ell}$ is the space derivative of $\zeta_{u}^{n,\ell}$ along certain direction. By (5.3b), we can similarly define

$$\left(\widetilde{\Phi_{\kappa}^{n,\ell}}, v\right) = \left(\eta_{q_\kappa}^{n,\ell}, v\right) + \mathcal{H}_{\kappa}^{\theta_\kappa}(\eta_{u}^{n,\ell}, v) + \mathcal{H}_{\kappa}^{\theta_\kappa}(e_{u}^{0}, v), \quad \forall\, v \in V_h, \tag{5.32}$$

for the fully-discrete LDG(I) scheme, and define

$$\left(\widetilde{\Phi_{\kappa}^{n,\ell}}, v\right) = \left(\eta_{q_\kappa}^{n,\ell}, v\right) + \mathcal{H}_{\kappa}^{\theta_\kappa}(\eta_{u}^{n,\ell}, v), \quad \forall\, v \in V_h, \tag{5.33}$$

for the fully-discrete LDG(II) scheme.

Repeating the similar discussion as that in the previous subsection, we use Lemma 5.3 and the approximation property to get that

$$\|\xi_{uq}^{n+1}\|_{\mu} \le CB(1+T)\left[h^{k+1} + \varrho h^{k} + \tau^{3}\right], \quad \forall\, n : n\tau \le T, \tag{5.34}$$

where the bounding constant $C > 0$ is independent of $n, h, \tau, \varepsilon^{-1}, \mu^{-1}$ and T. Finally, by using the triangle inequality and the approximation property again, we can complete the proof of Theorem 5.2.

6 Numerical Experiments

In this section, some numerical experiments are given to show that the presented error estimates are valid and sharp.

Example 1 Let $\Omega \in (0, 2\pi)^2$ and $T = 0.5$. Consider two-dimensional linear Sobolev equation (1.1) with the source term, namely

$$U_t + U_x + U_y - \varepsilon(U_{xx} + U_{yy}) = \mu(U_{xxt} + U_{yyt}) + F. \tag{6.1}$$

Let $U(x, y, t) = \sin(t+2)\sin(x)\sin(y)$ be the exact solution, and the initial solution and the source term F can be determined.

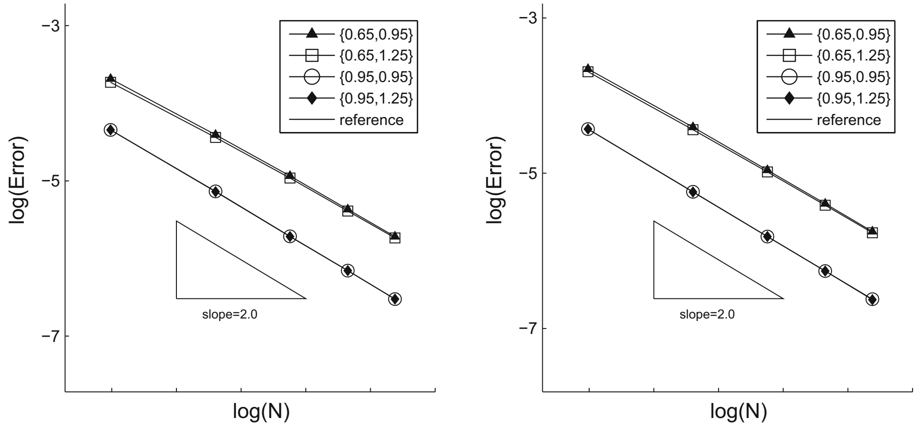

(a)

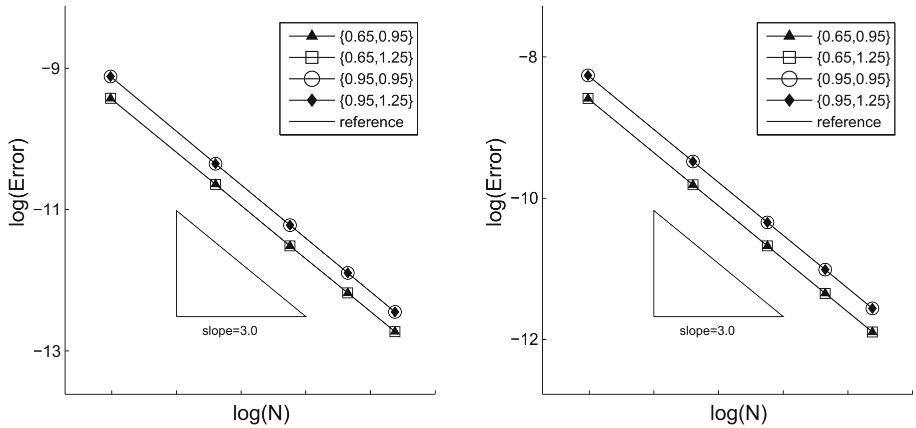

(b)

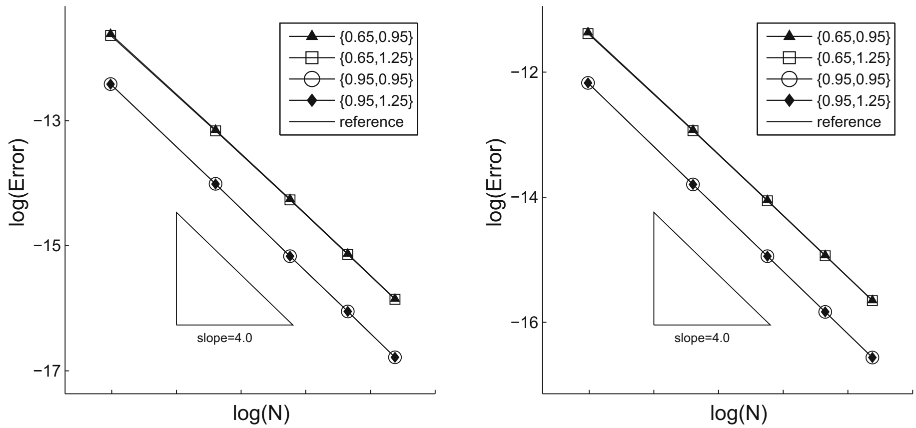

(c)

Fig. 1 Convergence orders in L^{∞}-norm (left) and L^2-norm (right): Example 1, $\varepsilon = \mu = 3$. **a** $k = 1$. **b** $k = 2$. **c** $k = 3$

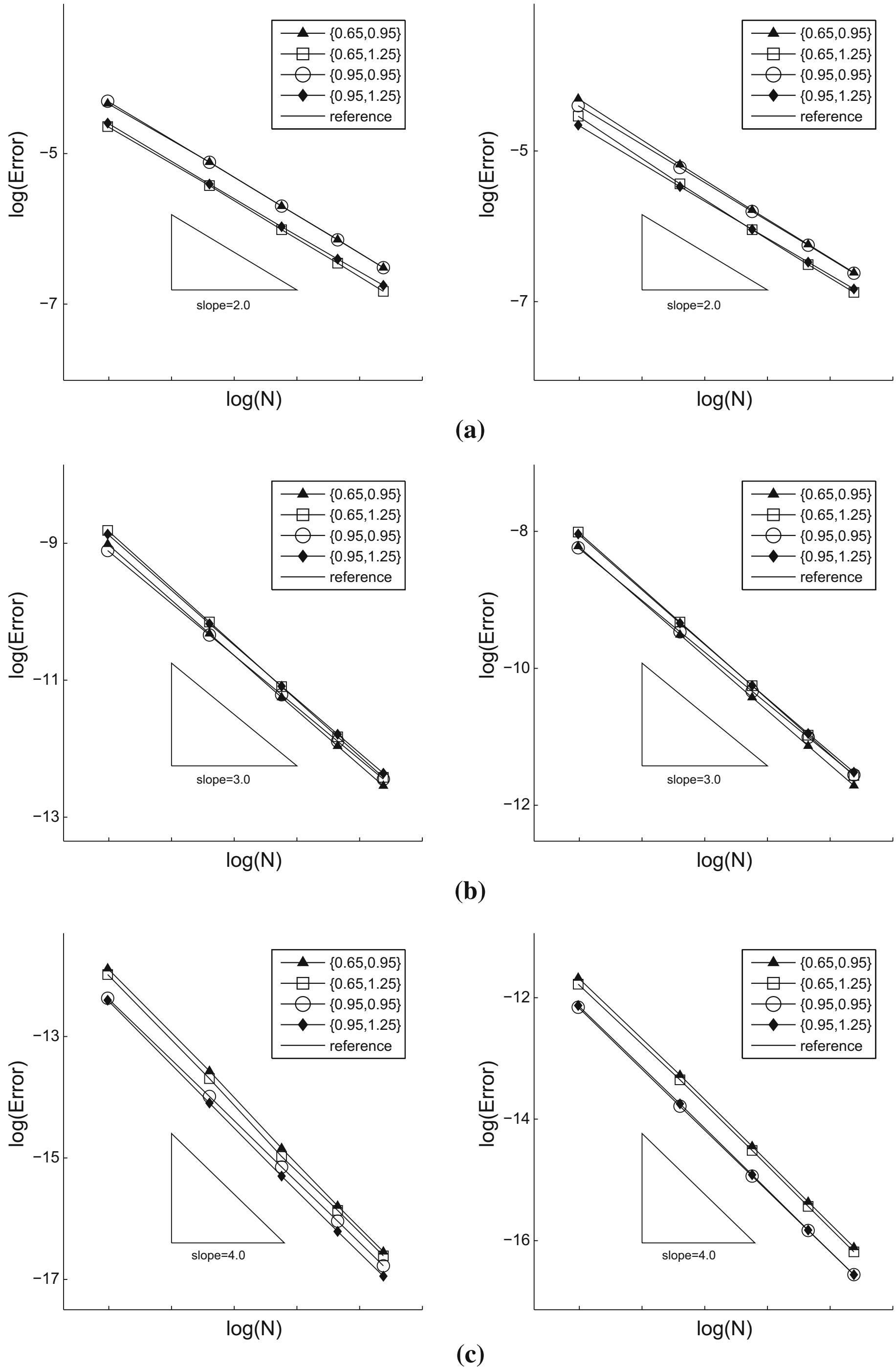

Fig. 2 Convergence orders in L^∞-norm (left) and L^2-norm (right): Example 1, $\varepsilon = \mu = 0.01$. **a** $k = 1$. **b** $k = 2$. **c** $k = 3$

The space domain is partitioned into $N \times N$ uniform squares, with the length $h = 2\pi/N$. The finite element space V_h is made up of $\mathcal{Q}_k$ elements with $k = 1, 2, 3$. The time step is taken small enough, such that the spatial error is dominated. The parameters in the generalized numerical fluxes are given in the following table:

$\theta_1 = \theta_2 = \theta$	0.65	0.65	0.95	0.95
$\gamma_1 = \gamma_2 = \gamma$	0.95	1.25	0.95	1.25

Since the numerical results are almost the same for both LDG schemes, we only present those for the fully-discrete LDG(I) scheme. The convergence orders of $u - U$ in L^2-norm and L^∞-norm are plotted, where N is equal to 20, 30, 40, 50 and 60. The diffusion and dispersion coefficients are taken $\varepsilon = \mu = 3$ in Fig. 1, and $\varepsilon = \mu = 0.01$ in Fig. 2, respectively. The optimal convergence orders are observed for different (θ, γ), hence the result in Theorem 5.2 is verified.

We also make a more deep investigation on the LDG schemes by taking $\varepsilon = \mu = 0.2$. In the same mesh refining as above, the diffusion and dispersion coefficients are considered to be at the same order as the mesh size. When $\theta_\kappa = \gamma_\kappa$, the optimal error order are still observed for arbitrary k, as we have shown in Theorem 5.2. To save space, we omit the data for this case and only show the numerical results when $\theta_\kappa \neq \gamma_\kappa$. For example, we take $\theta_\kappa = 0.65$ and $\gamma_\kappa = 1.25$. The errors and error orders in L^2-norm and L^∞-norm, for $k = 1, 2, 3$, are listed in Table 2. A half-order reduction is clearly observed for odd k, hence the result in Theorem 5.2 is sharp in this sense.

Example 2 In this example we investigate the stability performance for the LDG(I) scheme and the LDG(II) scheme.

To that end, we take $c_\kappa = 1, \varepsilon = 0$ and $\mu = 1$ in (1.1), where the μ-norms of exact solution are preserved for any time. Let the initial solution be $U_0(x, y) = \sin(2x + 2y)$, and take $N = 10$ and $k = 1$ in the numerical test. The μ-norms of numerical solutions at different time level are plotted in Fig. 3, where $\theta_\kappa = 0.65$, and $\gamma_\kappa = 0.5, 0.65, 0.95$ and

Table 2 Errors and error orders with $(\theta_\kappa, \gamma_\kappa) = (0.65, 1.25)$: Example 1

	N	$k = 1$		$k = 2$		$k = 3$	
		Error	Order	Error	Order	Error	Order
L^2-norm	20	1.44e−2		1.96e−4		8.26e−6	
	30	6.79e−2	1.86	5.66e−5	3.06	1.81e−6	3.74
	40	4.14e−3	1.72	2.36e−5	3.04	6.16e−7	3.75
	50	2.85e−3	1.67	1.20e−5	3.03	2.65e−7	3.78
	60	2.10e−3	1.67	6.93e−6	3.02	1.32e−7	3.80
L^∞-norm	20	1.20e−2		8.51e−5		5.26e−6	
	30	6.35e−3	1.57	2.48e−5	3.05	1.26e−6	3.52
	40	4.09e−3	1.52	1.03e−5	3.04	4.55e−7	3.55
	50	2.88e−3	1.58	5.25e−6	3.02	2.01e−7	3.66
	60	2.16e−3	1.58	3.03e−6	3.03	1.03e−7	3.69

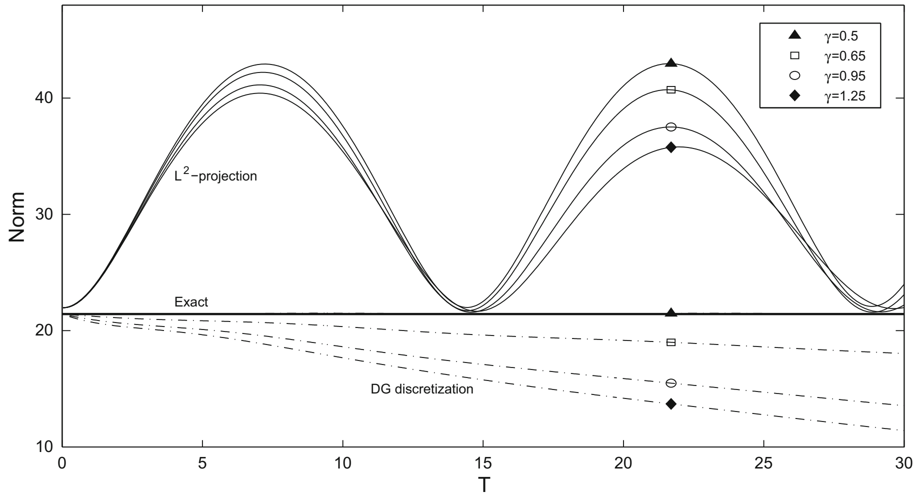

Fig. 3 The numerical performances for different setting of initial solutions

1.25, respectively, are taken in the numerical fluxes. The L^2*-projection* cure is for the LDG(I) scheme, where the μ-norms are not smaller than that in the initial time, however, they are still bounded with an oscillation. The *DG discretization* cure is for the LDG(II) scheme, where the decreasing μ-norms imply the strong stability as we have shown in Theorem 5.1. This numerical phenomenon shows the evident difference due to the setting of initial solutions.

Example 3 The LDG scheme presented in this paper can be easily extended to the nonlinear problem, for example,

$$U_t + f(U)_x + g(U)_y - \varepsilon(U_{xx} + U_{yy}) - \mu(U_{xxt} + U_{yyt}) = F. \tag{6.2}$$

Let $f(U) = g(U) = U^2/2$ and take $\varepsilon = \mu = 0.01$. The exact solution is given as $U(x, y, t) = \sin(x + y - 2t) + 2$, and the initial solution and the source term F can be determined by this solution. This time interval is $[0, 0.5]$.

We carry out the LDG(I) scheme to solve this problem, where the numerical fluxes for the nonlinear convection term are defined in a trivial extension

$$\widehat{f}_{i+\frac{1}{2},y} = f(\{\{u\}\}^{\gamma_1,y}_{i+\frac{1}{2},y}), \quad \widehat{g}_{x,j+\frac{1}{2}} = g\left(\{\{u\}\}^{x,\gamma_2}_{x,j+\frac{1}{2}}\right),$$

and the numerical fluxes for diffusion and dispersion are defined as before. In the numerical experiments, the parameters $(\theta_\kappa, \gamma_\kappa)$ are taken the same values as those in Example 1. The convergence orders of $u - U$ in L^2-norm and L^∞-norm, for $k = 1, 2, 3$, are plotted in Fig. 4. The optimal convergence orders are also observed.

7 Concluding Remarks

In this paper we present an efficient and high-order LDG method for two-dimensional linear Sobolev equation by introducing a special equivalent differential system. When the generalized alternating numerical fluxes are adopted, the stability result and error estimate are

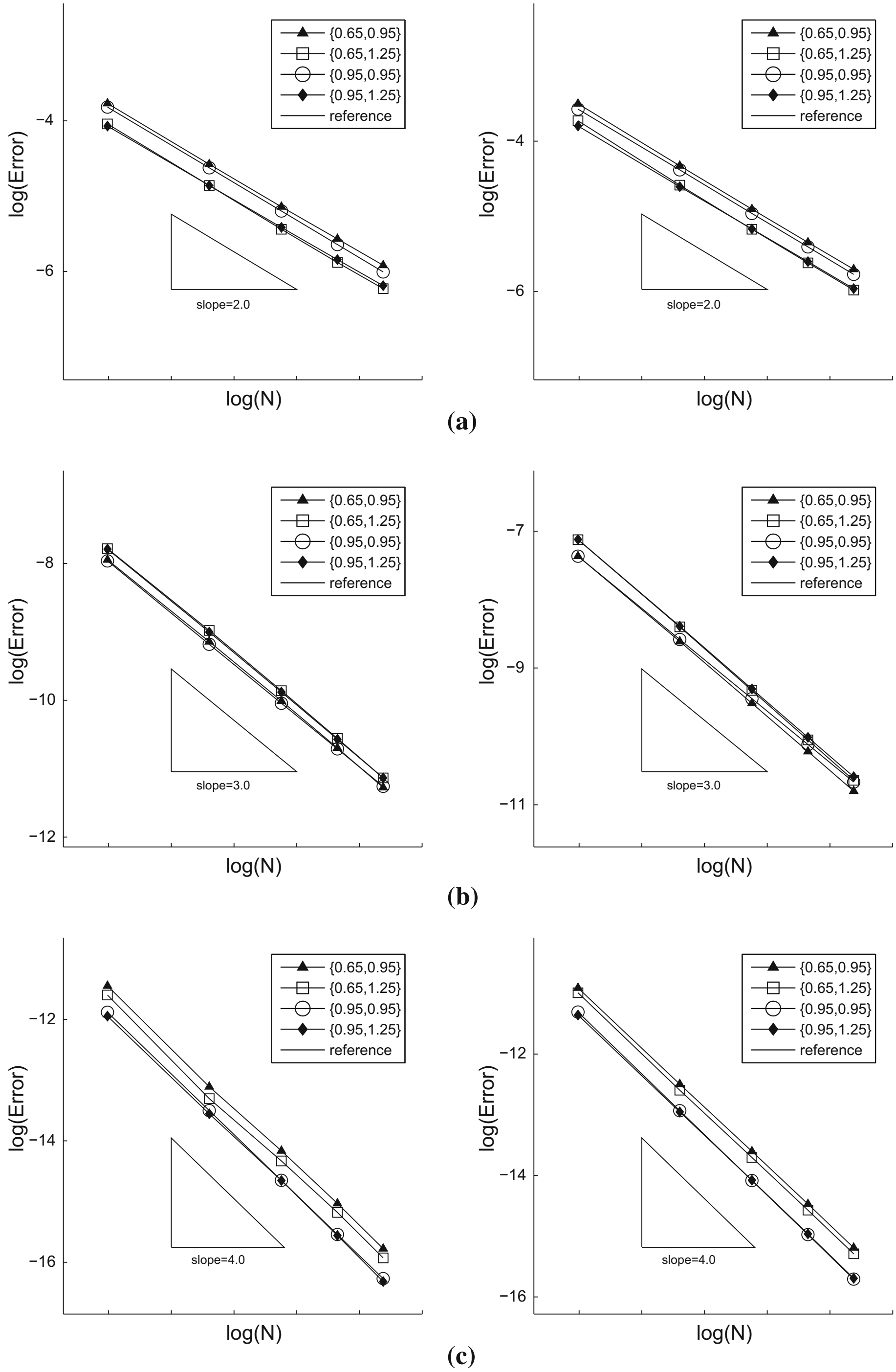

Fig. 4 Convergence orders in L^∞-norm (left) and L^2-norm (right): Example 3. **a** $k = 1$. **b** $k = 2$. **c** $k = 3$

presented for the semi-discrete scheme and fully-discrete scheme with the third order explicit TVDRK time-marching, respectively. The theory results hold no matter whether the viscosity coefficient and dispersion coefficient goes to zero, and the sharp error estimate is obtained by an elaborate application of the generalized Gauss–Radau projection. In the ongoing work, we will extend the above work to those partial differential equations involving mixed space–time derivatives of more higher order.

8 Appendix

In this section some detailed proofs for main conclusions are presented.

8.1 Proof of Lemma 5.2

By some certain linear combinations with three equations from (5.1a) to (5.1c), we can yield that

$$\left\langle \mathbb{D}_{\ell+1}\boldsymbol{z}_{uq}^n, \boldsymbol{v}_{uq} \right\rangle = \frac{\tau}{\ell+1}\left\langle \mathbb{D}_\ell \boldsymbol{z}_{wp}^n + \mathbb{D}_\ell \boldsymbol{\Psi}_{uq}^n, \boldsymbol{v}_{uq} \right\rangle, \quad \forall\, \boldsymbol{v}_{uq} \in (V_h)^3. \tag{8.1}$$

This relationship among the difference of stage solutions will be used many times

Below we take $\ell = 2$ as an example to prove this lemma. By taking $\boldsymbol{v}_{uq} = \mathbb{D}_3\boldsymbol{z}_{uq}^n$ in (8.1), we have

$$3\|\mathbb{D}_3\boldsymbol{z}_{uq}^n\|_\mu^2 = \tau\left\langle \mathbb{D}_2\boldsymbol{z}_{wp}^n + \mathbb{D}_2\boldsymbol{\Psi}_{uq}^n, \mathbb{D}_3\boldsymbol{z}_{uq}^n \right\rangle \le \|\mathbb{D}_3\boldsymbol{z}_{uq}^n\|_\mu^2 + \frac{\tau^2}{2}\|\mathbb{D}_2\boldsymbol{z}_{wp}^n\|_\mu^2 + \frac{\tau^2}{2}\|\mathbb{D}_2\boldsymbol{\Psi}_{uq}^n\|_\mu^2,$$

which implies that

$$\|\mathbb{D}_3\boldsymbol{z}_{uq}^n\|_\mu^2 \le \frac{\tau^2}{4}\|\mathbb{D}_2\boldsymbol{z}_{wp}^n\|_\mu^2 + \frac{\tau^2}{4}\|\mathbb{D}_2\boldsymbol{\Psi}_{uq}^n\|_\mu^2. \tag{8.2}$$

Take $\boldsymbol{v}_{wp} = \mathbb{D}_2\boldsymbol{z}_{wp}^n$ in (5.1d) for $\ell = 0, 1, 2$. A linear combination gives the identity

$$\|\mathbb{D}_2\boldsymbol{z}_{wp}^n\|_\mu^2 = \Lambda_1 + \Lambda_2 + \Lambda_3 + \Lambda_4,$$

where each term is given and estimated as follows:

$$\Lambda_1 = \sum_{\kappa=1}^{2} c_\kappa \mathcal{H}_\kappa^{\theta_\kappa}(\mathbb{D}_2 u^n, \mathbb{D}_2 w^n) \le 2M^2|c|^2h^{-2}\|\mathbb{D}_2 u^n\|^2 + \frac{1}{4}\|\mathbb{D}_2\boldsymbol{z}_{wp}^n\|_\mu^2, \tag{8.3a}$$

$$\Lambda_2 = -\varepsilon\sum_{\kappa=1}^{2}\mathcal{H}_\kappa^{1-\theta_\kappa}(\mathbb{D}_2 q_\kappa^n, \mathbb{D}_2 w^n) \le 2M^2\varepsilon^2h^{-2}\sum_{\kappa=1}^{2}\|\mathbb{D}_2 q_\kappa^n\|^2 + \frac{1}{4}\|\mathbb{D}_2\boldsymbol{z}_{wp}^n\|_\mu^2, \tag{8.3b}$$

$$\Lambda_3 = -\mu\sum_{\kappa=1}^{2}\left[\mathcal{H}_\kappa^{1-\theta_\kappa}(\mathbb{D}_2 p_\kappa^n, \mathbb{D}_2 w^n) + \mathcal{H}_\kappa^{\theta_\kappa}(\mathbb{D}_2 w^n, \mathbb{D}_2 p_\kappa^n)\right] = 0, \tag{8.3c}$$

$$\Lambda_4 = \left\langle \mathbb{D}_2\boldsymbol{\Psi}_{wp}^n, \mathbb{D}_2\boldsymbol{z}_{wp}^n \right\rangle \le \|\mathbb{D}_2\boldsymbol{\Psi}_{wp}^n\|_\mu^2 + \frac{1}{4}\|\mathbb{D}_2\boldsymbol{z}_{wp}^n\|_\mu^2. \tag{8.3d}$$

In the above process, the boundedness property (Lemma 3.3) and the skew-symmetrical property (Lemma 3.1) of DG discretization are used. Finally, collecting up the above conclusion completes the proof of this lemma.

8.2 Proof of (5.9)

Firstly in (5.4) we take $v = -\varepsilon q_\kappa^{n,\ell}$ and $v = -\mu p_\kappa^{n,\ell}$. Then in (5.1d) we take $\boldsymbol{v}_{wp} = (u^{n,\ell}, 0, 0)$. Summing up the resulting equations, we have

$$\mathcal{R}_1^n = \sum_{\ell=0}^{2} d_\ell \Big[\mathcal{R}_{11}^{n,\ell} + \mathcal{R}_{12}^{n,\ell} + \mathcal{R}_{13}^{n,\ell} + \mathcal{R}_{14}^{n,\ell} + \mathcal{R}_{15}^{n,\ell}\Big]\tau, \tag{8.4}$$

Each term in (8.4) is given and bounded as follows:

$$\mathcal{R}_{11}^{n,\ell} = \sum_{\kappa=1}^{2} c_\kappa \mathcal{H}_\kappa^{\gamma_\kappa}(u^{n,\ell}, u^{n,\ell}) = -\frac{1}{2}\sum_{\kappa=1}^{2} c_\kappa(2\gamma_\kappa - 1)\|[\![u^{n,\ell}]\!]\|_{\Gamma_h^\kappa}^2, \tag{8.5a}$$

$$\mathcal{R}_{12}^{n,\ell} = -\varepsilon \sum_{\kappa=1}^{2} \Big[\mathcal{H}_\kappa^{1-\theta_\kappa}(q_\kappa^{n,\ell}, u^{n,\ell}) + \mathcal{H}_\kappa^{\theta_\kappa}(u^{n,\ell}, q_\kappa^{n,\ell})\Big] = 0, \tag{8.5b}$$

$$\mathcal{R}_{13}^{n,\ell} = -\mu \sum_{\kappa=1}^{2} \Big[\mathcal{H}_\kappa^{1-\theta_\kappa}(p_\kappa^{n,\ell}, u^{n,\ell}) + \mathcal{H}_\kappa^{\theta_\kappa}(u^{n,\ell}, p_\kappa^{n,\ell})\Big] = 0, \tag{8.5c}$$

$$\mathcal{R}_{14}^{n,\ell} = -\varepsilon \sum_{\kappa=1}^{2} \Big(q_\kappa^{n,\ell}, q_\kappa^{n,\ell}\Big), \tag{8.5d}$$

$$\mathcal{R}_{15}^{n,\ell} = \sum_{\kappa=1}^{2} \Big(\Phi_\kappa^{n,\ell}, \varepsilon q_\kappa^{n,\ell} + \mu p_\kappa^{n,\ell}\Big) + \Big(\Psi_w^{n,\ell}, u^{n,\ell}\Big) + \Big\langle \boldsymbol{\Psi}_{uq}^{n,\ell}, z_{uq}^{n,\ell}\Big\rangle. \tag{8.5e}$$

The first one is resulted from Lemma 3.2, and the next two are resulted from Lemma 3.1. Till now we have obtained (5.9).

8.3 Proof of (5.10)

In (8.1) we take $\boldsymbol{v}_{uq} = (\mathbb{D}_2 u^n, 0, 0)$ for $\ell = 1$ and $\boldsymbol{v}_{uq} = (\mathbb{D}_1 u^n, 0, 0)$ for $\ell = 2$. Noticing (5.1d) with the same test functions, we obtain the identity

$$\mathcal{R}_2^n = \mathcal{R}_{21}^n\tau + \mathcal{R}_{22}^n\tau + \mathcal{R}_{23}^n\tau + \mathcal{R}_{24}^n\tau + \Theta_{21}^n\tau, \tag{8.6}$$

where

$$\mathcal{R}_{21}^n = \sum_{\kappa=1}^{2} c_\kappa \Big[\mathcal{H}_\kappa^{\gamma_\kappa}(\mathbb{D}_1 u^n, \mathbb{D}_2 u^n) + \mathcal{H}_\kappa^{\gamma_\kappa}(\mathbb{D}_2 u^n, \mathbb{D}_1 u^n)\Big], \tag{8.7a}$$

$$\mathcal{R}_{22}^n = -\varepsilon \sum_{\kappa=1}^{2} \Big[\mathcal{H}_\kappa^{1-\theta_\kappa}(\mathbb{D}_1 q_\kappa^n, \mathbb{D}_2 u^n) + \mathcal{H}_\kappa^{1-\theta_\kappa}(\mathbb{D}_2 q_\kappa^n, \mathbb{D}_1 u^n)\Big], \tag{8.7b}$$

$$\mathcal{R}_{23}^n = -\mu \sum_{\kappa=1}^{2} \Big[\mathcal{H}_\kappa^{1-\theta_\kappa}(\mathbb{D}_1 p_\kappa^n, \mathbb{D}_2 u^n) + \mathcal{H}_\kappa^{1-\theta_\kappa}(\mathbb{D}_2 p_\kappa^n, \mathbb{D}_1 u^n)\Big], \tag{8.7c}$$

$$\mathcal{R}_{24}^n = \mu \sum_{\kappa=1}^{2} \Big[\Big(\mathbb{D}_1 p_\kappa^n, \mathbb{D}_2 q_\kappa^n\Big) + \Big(\mathbb{D}_2 p_\kappa^n, \mathbb{D}_1 q_\kappa^n\Big)\Big]. \tag{8.7d}$$

Each term can be estimated one by one.

Combining Lemma 3.2, Young's inequality and the inverse property, we yield that

$$\begin{aligned}\mathcal{R}_{21}^n &\leq \sum_{\kappa=1}^{2} c_\kappa(2\gamma_\kappa-1)\Big[2\|[\![\mathbb{D}_2u^n]\!]\|_{\Gamma_h^\kappa}^2+\frac{1}{8}\|[\![\mathbb{D}_1u^n]\!]\|_{\Gamma_h^\kappa}^2\Big]\\ &\leq 4\nu^2h^{-1}\sum_{\kappa=1}^{2} c_\kappa(2\gamma_\kappa-1)\|\mathbb{D}_2\boldsymbol{z}_{uq}^n\|_\mu^2+\sum_{\ell=0}^{1}\sum_{\kappa=1}^{2}\frac{1}{4}d_\ell c_\kappa(2\gamma_\kappa-1)\|[\![u^{n,\ell}]\!]\|_{\Gamma_h^\kappa}^2.\end{aligned} \tag{8.8}$$

Taking $v=-\varepsilon\mathbb{D}_1q_\kappa^n$ and $v=-\varepsilon\mathbb{D}_2q_\kappa^n$ in (5.4) with $\ell=0,1,2$, and adding the resulted identities into $\mathcal{R}_{22}^n$ with suitable weight, we can get

$$\mathcal{R}_{22}^n=\mathcal{R}_{221}^n+\mathcal{R}_{222}^n+\mathcal{R}_{223}^n+\Theta_{22}^n, \tag{8.9}$$

where each term is given and/or estimated as follows:

$$\mathcal{R}_{221}^n = -\varepsilon\sum_{\kappa=1}^{2}\Big[\mathcal{H}_\kappa^{1-\theta_\kappa}(\mathbb{D}_1q_\kappa^n,\mathbb{D}_2u^n)+\mathcal{H}_\kappa^{\theta_\kappa}(\mathbb{D}_2u^n,\mathbb{D}_1q_\kappa^n)\Big]=0, \tag{8.10a}$$

$$\mathcal{R}_{222}^n = -\varepsilon\sum_{\kappa=1}^{2}\Big[\mathcal{H}_\kappa^{1-\theta_\kappa}(\mathbb{D}_2q_\kappa^n,\mathbb{D}_1u^n)+\mathcal{H}_\kappa^{\theta_\kappa}(\mathbb{D}_1u^n,\mathbb{D}_2q_\kappa^n)\Big]=0, \tag{8.10b}$$

$$\mathcal{R}_{223}^n = -2\varepsilon\sum_{\kappa=1}^{2}\Big[\Big(\mathbb{D}_2q_\kappa^n,\mathbb{D}_1q_\kappa^n\Big)-\Big(\mathbb{D}_2\Phi_\kappa^n,\mathbb{D}_1q_\kappa^n\Big)\Big]. \tag{8.10c}$$

The first two conclusions are directly resulted from Lemma 3.1. Taking $v=-2\varepsilon\mathbb{D}_1q_\kappa$ in (5.4) with $\ell=0,1,2$, we can get that

$$\begin{aligned}\mathcal{R}_{223}^n&=2\varepsilon\sum_{\kappa=1}^{2}\mathcal{H}_\kappa^{\theta_\kappa}(\mathbb{D}_2u^n,\mathbb{D}_1q_\kappa^n)\leq 2M\varepsilon h^{-1}\sum_{\kappa=1}^{2}\|\mathbb{D}_2u^n\|\|\mathbb{D}_1q_\kappa^n\|\\ &\leq\frac{1}{4\tau}\|\mathbb{D}_2u^n\|^2+8M^2\varepsilon^2h^{-2}\tau\|\mathbb{D}_1\boldsymbol{q}^n\|^2\leq\frac{1}{4\tau}\|\mathbb{D}_2u^n\|^2+16M^2\varepsilon^2h^{-2}\sum_{\ell=0}^{1}d_\ell\|\boldsymbol{q}^{n,\ell}\|^2\tau.\end{aligned} \tag{8.11}$$

Collecting up the above analysis yields the estimate to $\mathcal{R}_{22}^n$.

Along the same line as before, it is easy to get that

$$\mathcal{R}_{23}^n+\mathcal{R}_{24}^n=\Theta_{23}^n. \tag{8.12}$$

Finally, summing up the above conclusions into (8.6), and noticing the definitions of $\lambda_\mathrm{c},\lambda_\mathrm{d},\mathcal{S}_\mathrm{c}$ and $\mathcal{S}_\mathrm{d}$, we can obtain (5.10).

References

1. Amiraliyev, G.M., Mamedov, Y.D.: Difference schemes on the uniform mesh for singular perturbed pseudo-parabolic equations. Turk. J. Math. **19**, 207–222 (1995)
2. Arnold, D.N., Douglas, J., Thomee, V.: Superconvergence of finite element approximation to the solution of a Sobolev equation in a single space variable. Math. Comput. **27**, 737–743 (1981)
3. Bassi, F., Rebay, S.: A high-order accurate discontinuous finite element method for the numerical solution of the compressible Navier–Stokes equations. J. Comput. Phys. **131**, 267–279 (1997)
4. Cheng, Y., Meng, X., Zhang, Q.: Application of generalized Gauss–Radau projections for the local discontinuous Galerkin methods for linear convection–diffusion equations. Math. Comput. **86**, 1233–1267 (2017)

5. Cockburn, B., Shu, C.W.: TVB Runge–Kutta local projection discontinuous Galerkin finite element method for conservation laws II: general framework. Math. Comput. **52**, 411–435 (1989)
6. Cockburn, B., Shu, C.W.: The Runge–Kutta discontinuous Galerkin finite element method for conservation laws V: multidimensional systems. J. Comput. Phys. **141**, 199–2224 (1998)
7. Cockburn, B., Shu, C.W.: The local discontinuous Galerkin method for time-dependent convection–diffusion systems. SIAM. J. Numer. Anal. **35**, 2440–2463 (1998)
8. Cockburn, B., Shu, C.W.: Runge–Kutta discontinuous Galerkin methods for convection-dominated problems. J. Sci. Comput. **16**, 173–261 (2001)
9. Davis, P.L.: A quasilinear parabolic and a related third order problem. J. Math. Anal. Appl. **40**, 327–335 (1972)
10. Esen, A., Kutluay, S.: Application of a lumped Galerkin method to the regularized long wave equation. Appl. Math. Comput. **174**, 485–494 (2001)
11. Ewing, R.E.: Numerical solution of Sobolev partial differential equations. SIAM J. Numer. Anal. **12**, 345–363 (1975)
12. Ewing, R.E.: A coupled non-linear hyperbolic-Sobolev system. Ann. Mat. Pure Appl. **114**, 331–349 (1977)
13. Ewing, R.E.: Time-stepping Galerkin methods for nonlinear Sobolev partial differential equation. SIAM. J. Numer. Anal. **15**, 1125–1150 (1978)
14. Gao, F.Z., Qiu, J.X., Zhang, Q.: Local discontinuous Galerkin finite element method and error estimates for one class of Sobolev equation. J. Sci. Comput. **41**, 436–460 (2009)
15. Guo, L., Chen, H.: H_1-Galerkin mixed finite element method for the regularized long wave equation. Computing **77**, 205–221 (2006)
16. Levy, D., Shu, C.W., Yan, J.: Local discontinuous Galerkin methods for nonlinear dispersive equations. J. Comput. Phys. **196**, 751–774 (2004)
17. Meng, X., Shu, C.W., Wu, B.: Optimal error estimates for discontinuous Galerkin methods based on upwind-biased fluxes for linear hyperbolic equations. Math. Comput. **85**, 1225–1661 (2016)
18. Omrani, K.: The convergence of the fully discrete Galerkin approximations for Benjamin–Bona–Mahony equation. Appl. Math. Comput. **180**, 614–621 (2006)
19. Pani, A.K., Fairweather, G.: H_1-Galerkin mixed finite element methods for parabolic partial integro-differential equations. IMAJ Numer. Anal. **22**, 231–252 (2002)
20. Xu, Y., Shu, C.W.: A local discontinuous Galerkin method for the Camassa–Holm equation. SIAM. J. Numer. Anal. **46**(4), 1998–2021 (2008)
21. Yan, J., Shu, C.W.: Local discontinuous Galerkin method for partial differential equations with higher order derivatives. J. Sci. Comput. **17**, 27–47 (2002)
22. Yan, J., Shu, C.W.: A local discontinuous Galerkin method for KdV type equations. SIAM. J. Numer. Anal. **40**, 769–791 (2002)
23. Zhang, Q., Gao, F.Z.: A fully-discrete local discontinuous Galerkin method for convection-dominated Sobolev equation. J. Sci. Comput. **51**(1), 107–134 (2012)
24. Zhang, Q., Shu, C.W.: Stability analysis and a priori error estimates of third order explicit Runge–Kutta discontinuous Galerkin method for scalar conservation laws. SIAM. J. Numer. Anal. **48**, 1038–1063 (2010)